Airflow visualization experiment and CFD analysis in mixed convection inside a rectangular riser

김신엽*

한국원자력연구원, 원자력수소연구실
서울대학교, 열수력연구실
* kimsy@kaeri.re.kr

2023.5.17.(수)

Introduction; motivation

Reactor Cavity Cooling System, RCCS

- Passive heat removal system of VHTR
- Rectangular channels
- Reduced scale experiment; KAERI, ANL, SNU, and so on

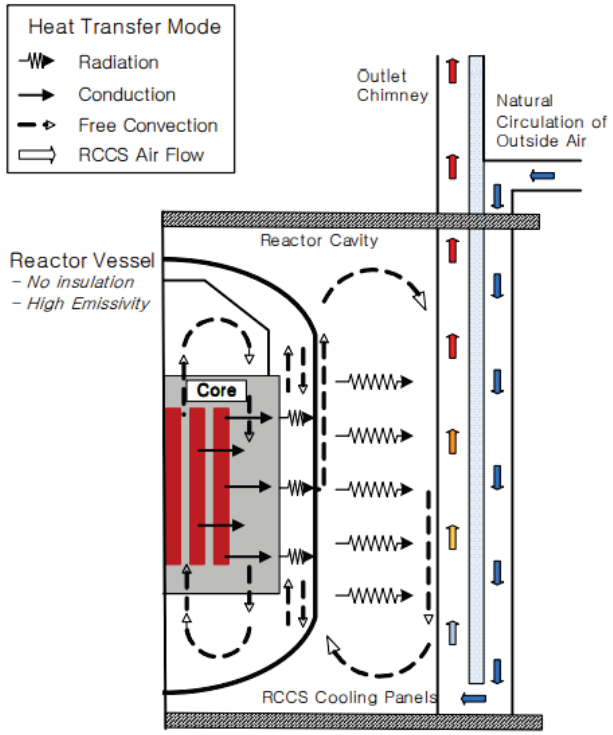

Reactor Cavity Cooling System (VHTR)
developed by KAERI. [J.-H. Kim et al., 2015]

Heat transfer deterioration under mixed convection

- Higher wall temperature than under forced convection
- Depending on the turbulence model, different predictions

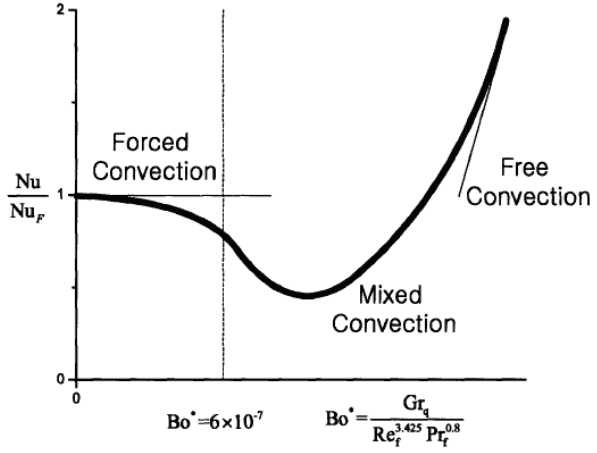

Mixed convection heat transfer correlation
[Jackson et al., 1989]

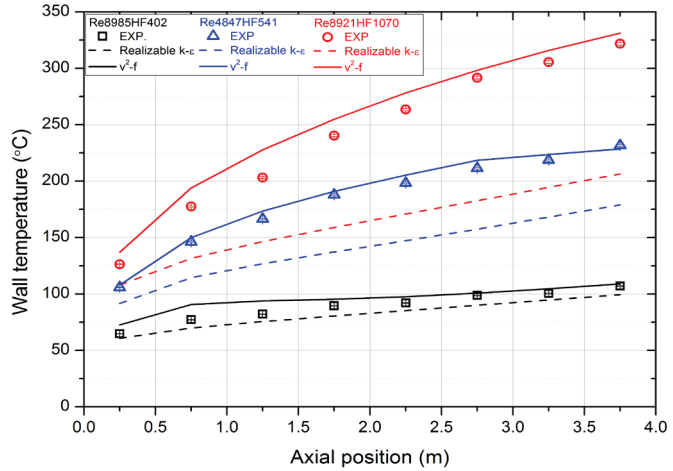

CFD analysis results for SNU-RHEF experimental conditions [Kim et al., 2021]

- ✓ Heat transfer mechanism needs to be investigated.
- ✓ Airflow visualization experiment

Introduction; Research works

Airflow visualization experiment and CFD analysis in mixed convection inside a rectangular riser

Airflow visualization experiment

- ✓ Experiment for a heated rectangular riser

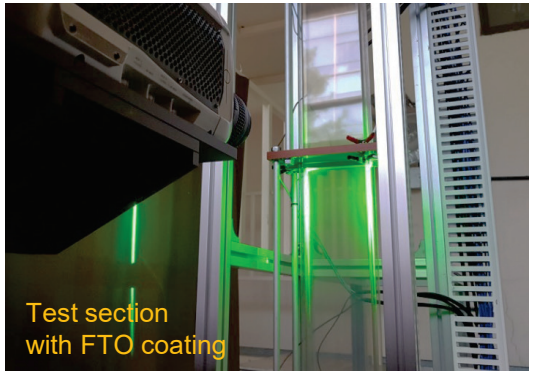

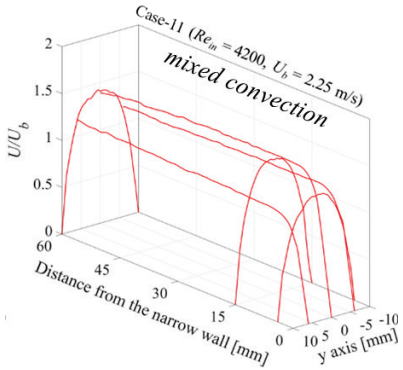

- ✓ CFD analyses with experimental conditions

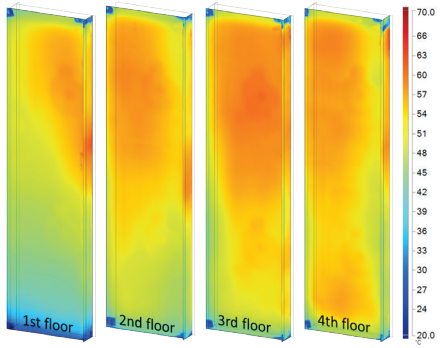

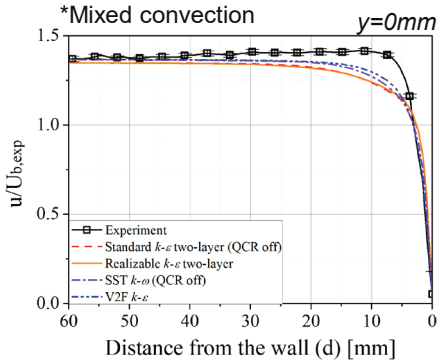

Modification of RANS turbulence model

- ✓ Heat transfer deterioration/enhancement under mixed convection

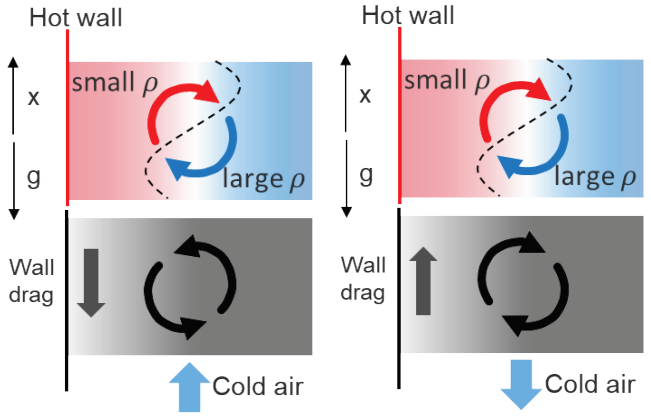

- ✓ Symmetrical flow characteristics along the corner bisector

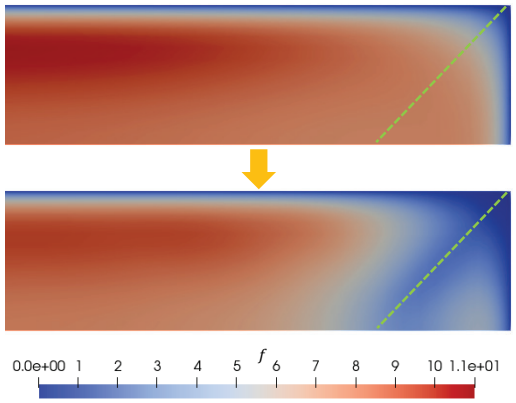

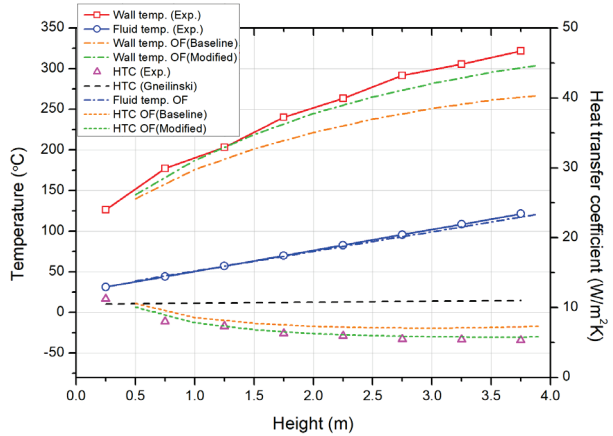

CONTENTS

Airflow visualization experiment

FROVE; Four-Side Heating Riser Flow Visualization Experiment Facility

- Transparent test section for flow visualization
  - Heating region: 2.0 m (≈ 60 D_h), Entrance region (PVC): 1.0 m (≈ 30 D_h)
    - Inner test section: 120 mm × 20 mm × 2000 mm
  - FTO (Fluorine doped Tin Oxide) coated heat-resistant glass
    - FTO: Transparent conducting material for resistive heating
    - Heating power ← Power supply, control panel (~ 300 °C)

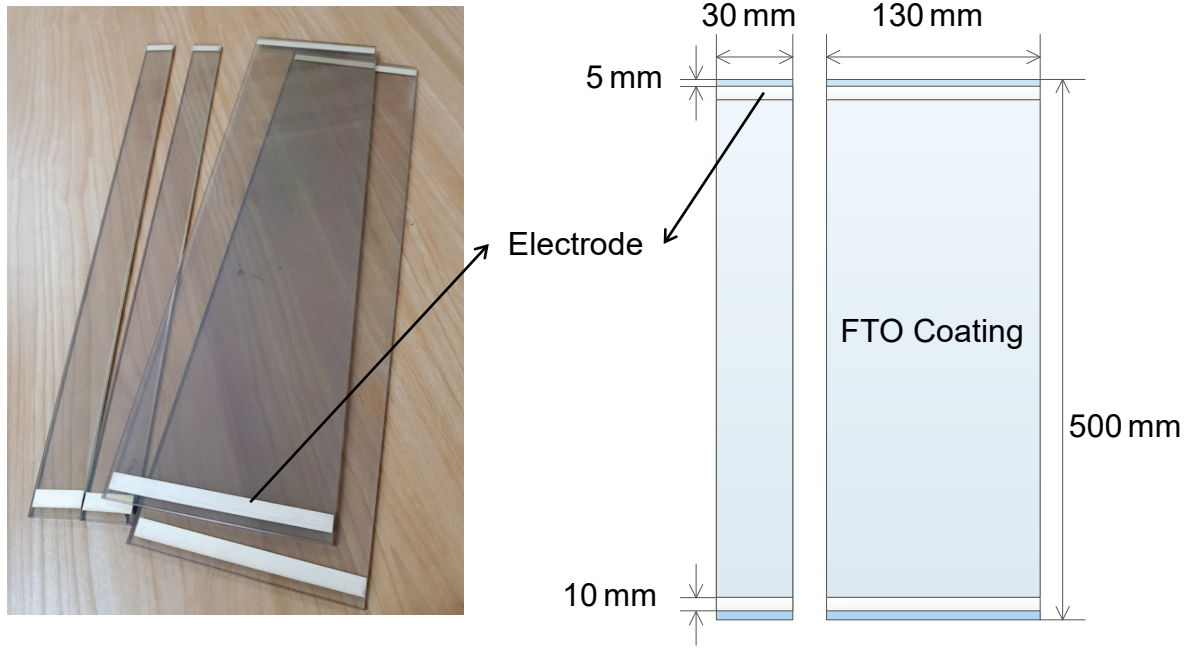

FTO coated heat-resistant glass and its design

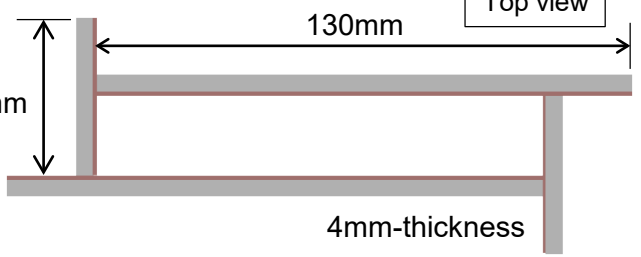

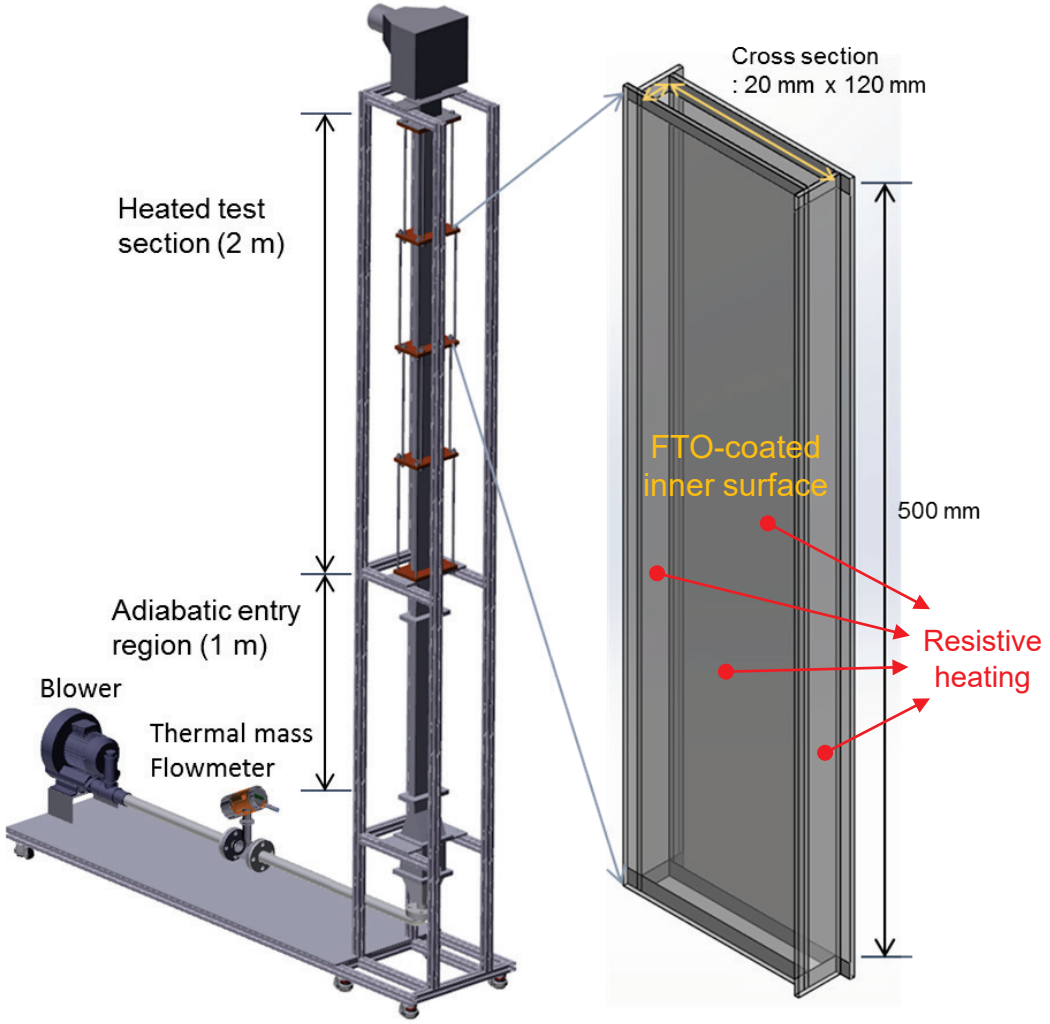

Schematics of airflow visualization experiment facility and its test section

Airflow visualization experiment

FROVE; Four-Side Heating Riser Flow Visualization Experiment Facility

- Upper plenum
  - Thermal insulation for quantification of heat removal
  - Total 10 thermo-couples were installed.

- ✓ **Lower plenum**
  - ✓ To match the inlet conditions with the CFD inlet conditions
    - 450 mm length, cross-section = 120 mm x 120 mm
  - Contraction ratio = inlet area / exit area = 6,
    lower than the recommended contraction [Abdelhamed et al., 2015]
  - Honeycomb
    : lateral flow uniformity [Kulkami et al., 2011]
    - Thickness: 0.5 T, mesh size: 10 mm x 10 mm, length: 100 mm
    - Based on the design criteria of the wind tunnel test standard (KS B 6311)
  - Perforated screens
    : lower lateral turbulence production [Scheiman and Brooks, 1981]
    - 8Ø * 12P, 60 degree

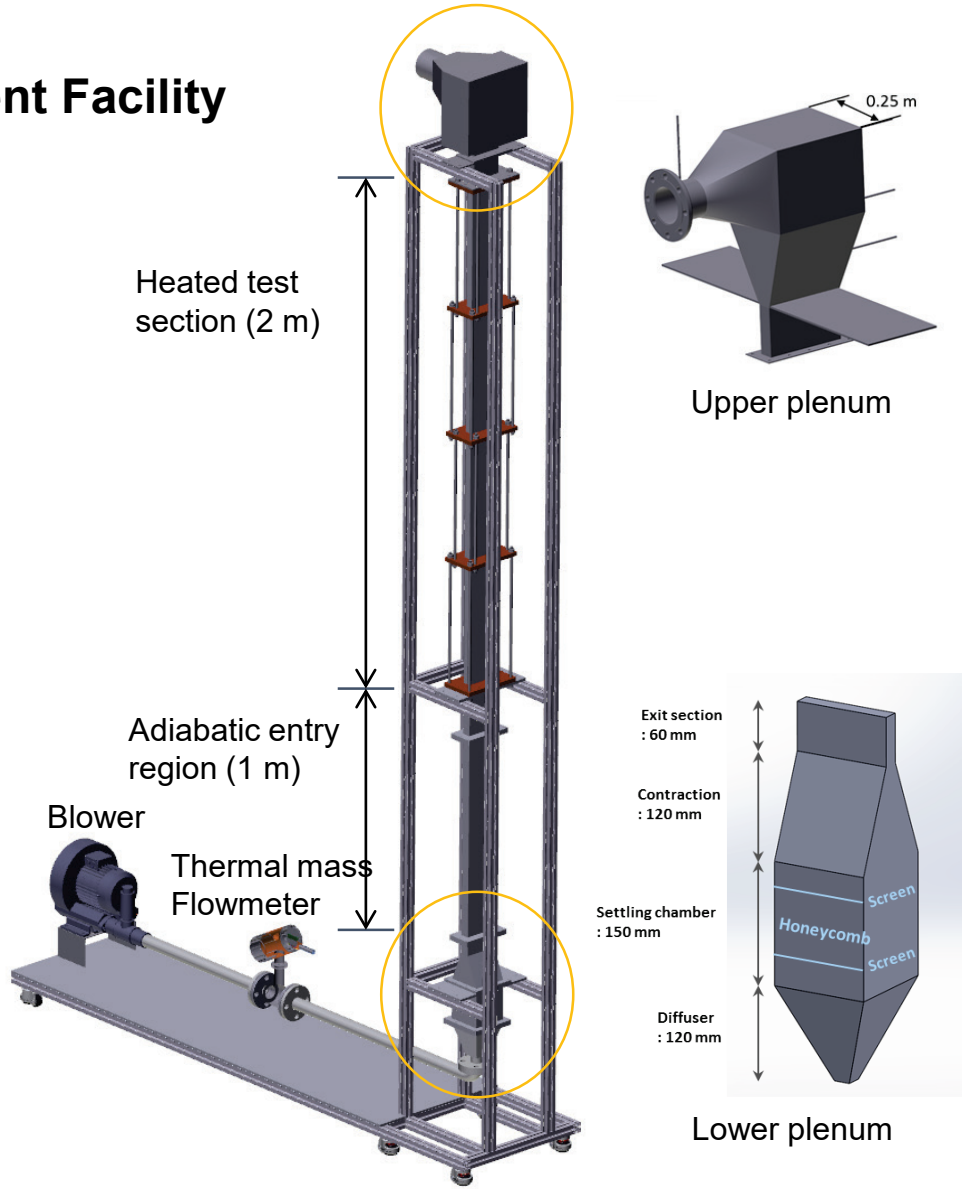

Schematics of airflow visualization experiment facility and its plenums

Measurement methods

Velocity field measurement

- PIV (Particle Image Velocimetry) method
  - Continuous laser and high speed camera on linear traverse system

- Seed particle for PIV method
  - DEHS (Di-Ethyl-Hexyle-Sebacat) aerosol
    - Non-toxic, volatile oil (boiling point: about 240 °C)
    - Droplet size: 1 μm-diameter
    - Mass fraction of DEHS to the air mass flow < 10^{-5}

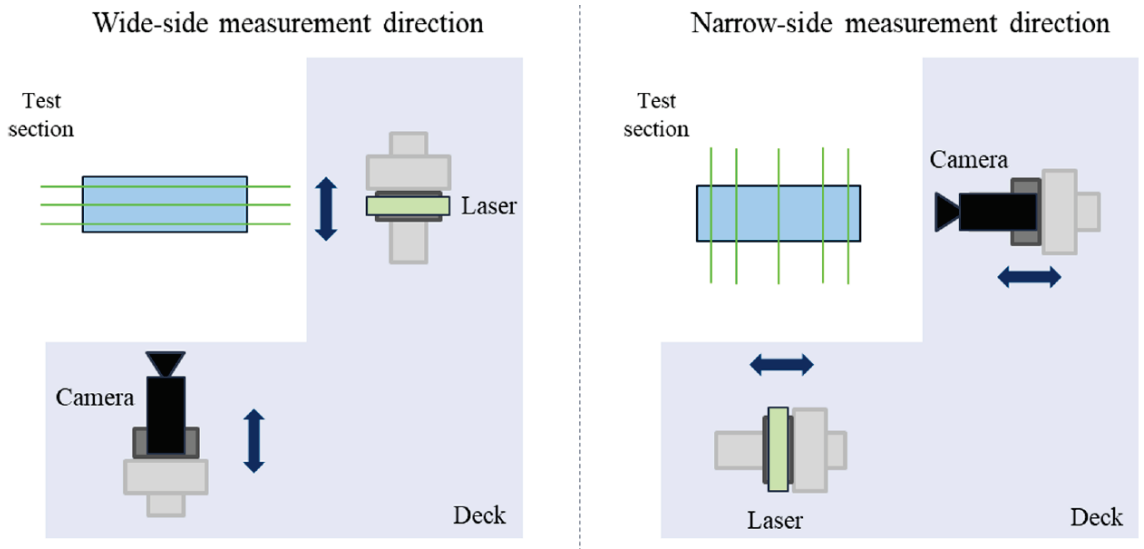

Velocity measurement strategy with two linear traverse systems

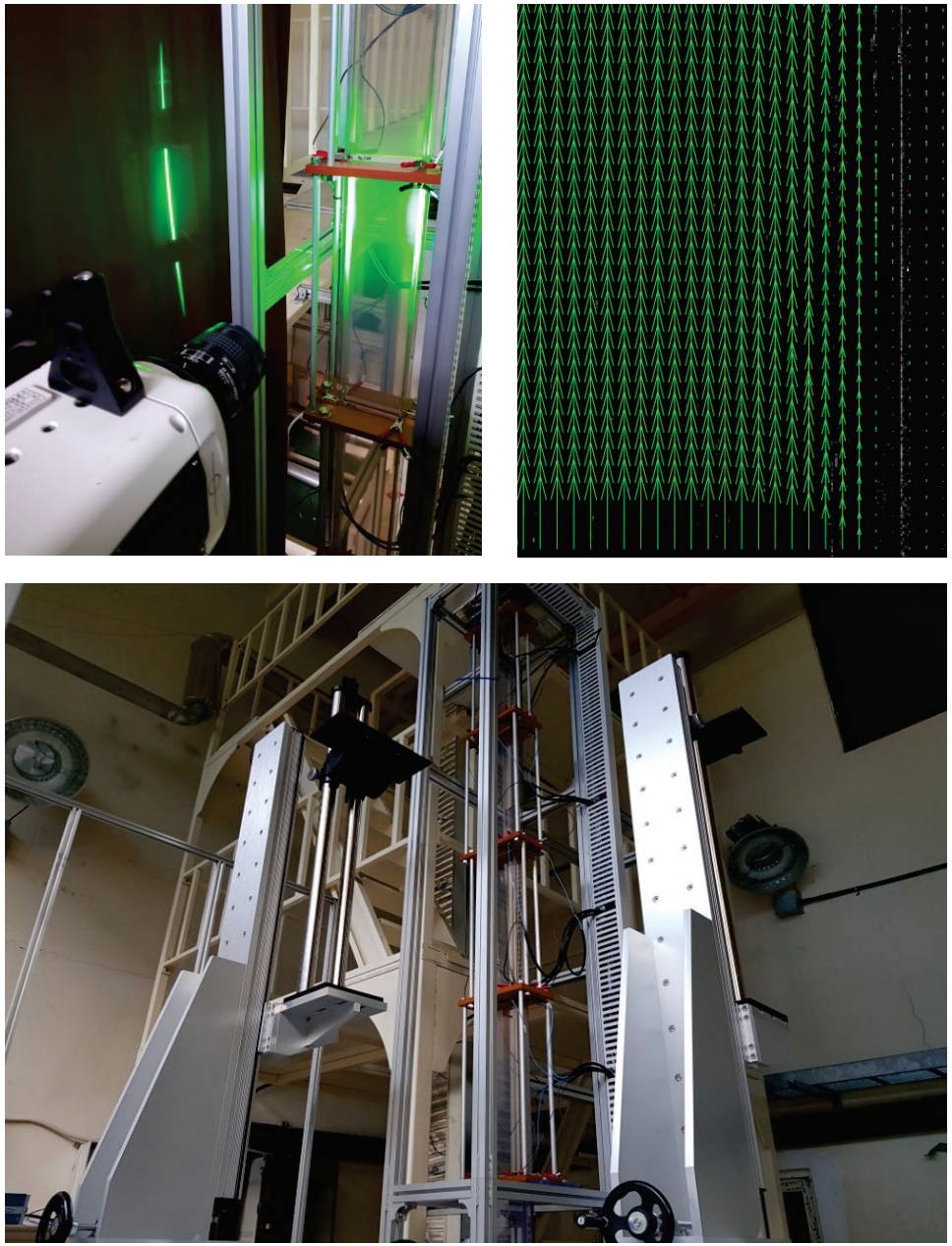

Pictures of FROVE and linear traverse system and PIV analysis result

Measurement methods

Flow traceability of seed particles

- Relaxation time of particle, τ_p
  - Response (or relaxation) time of a particle to a sudden change of the flow velocity
  - In this study, $d_p = 1\ \mu m, \rho_p = 912\ kg/m^3, \mu = 1.85 \times 10^{-5}\ kg/m \cdot s \rightarrow \tau_p = 2.7 \times 10^{-6}\ s$
- Stokes number, *St*

$$St = \tau_p \frac{U_f}{L} = \frac{\rho_p d_p^2 U_f}{18 \mu L}$$ (*L*: Characteristic length, typically, diameter)

  - In this study, $St \ll 0.1$, ensuring tracing accuracy errors below 1 %. [W. C. Hinds, 2012]

Mean droplet size
; $1\mu m$ for DEHS oil (typical)
Aerosol flow rate
; 30 LPM (normal operation)

TSI, Oil droplet generator, Model 9307

Enhancement of detectability of PIV analysis

- Pre-processing for PIV analysis [PIVlab]
  - Background subtraction
  - CLAHE
- Time averaged measurement variables
  - 60 seconds, 1500 velocity vector fields

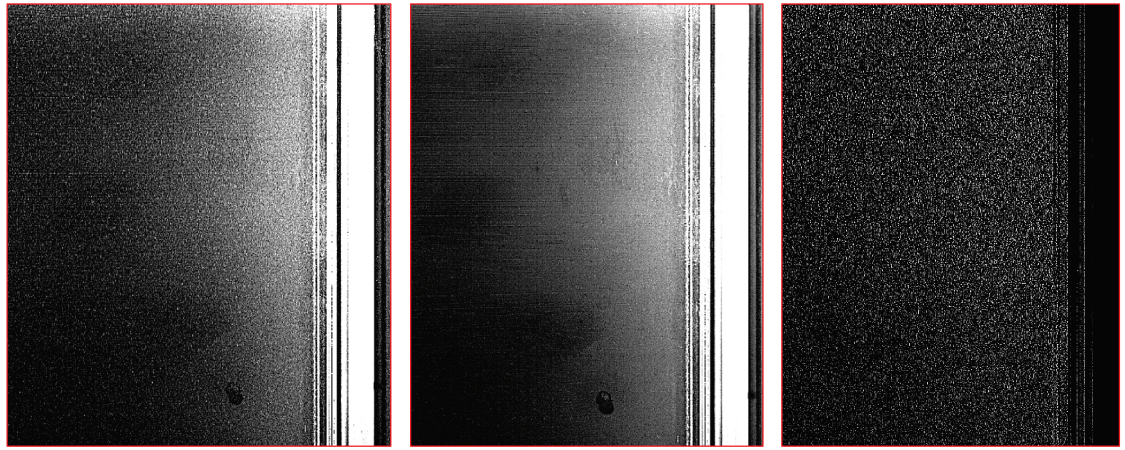

Raw image | Averaged image | Pre-processed image

PIV settings

Keane R.D. and Adrian R. J.
Optimization of particle image velocimeters, 1990
Theory of cross-correlation analysis of PIV images, 1992

Factors that affect the results of PIV analysis

- Primary factors: Velocity, velocity gradient, magnification, aperture (depth of field)
- Secondary factors: No. density of seed (N_I), time interval, exposure time, interrogation area (d_1)

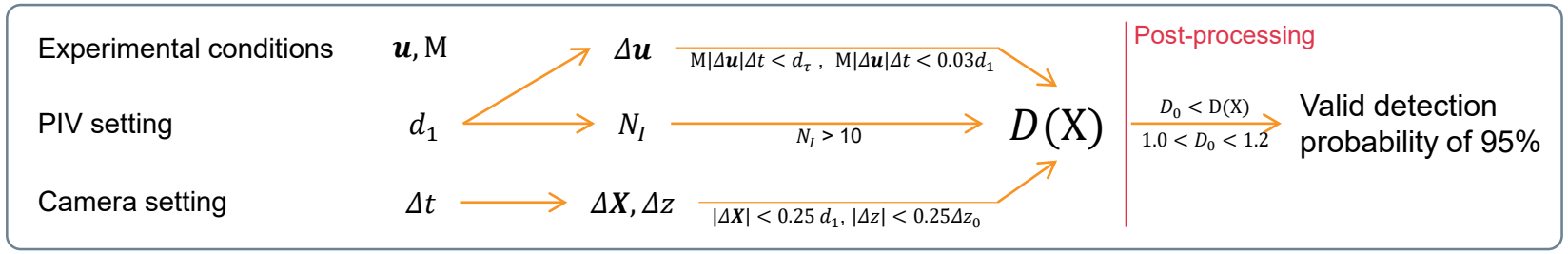

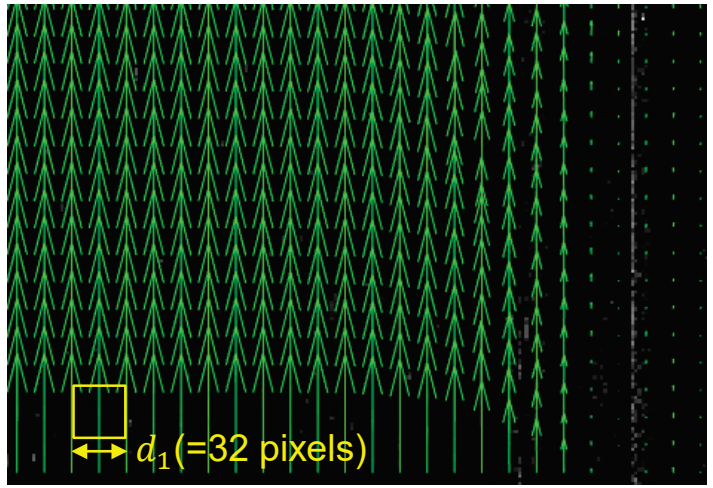

Considerations for the selection of camera and PIV settings

$N_I > 10 \longrightarrow d_{1,\min}$ $\qquad$ $|\Delta u_{\max}| \longrightarrow d_{1,\max}$

$|\Delta z| < 0.25 \Delta z_0 \longrightarrow \Delta t_{\max 1} = \dfrac{\Delta z_0}{4w}$ $\qquad$ $|\Delta \boldsymbol{X}| < 0.25\, d_1 \longrightarrow \Delta t_{\max 2} = \dfrac{d_{1,\max}}{4u}$

$\mathrm{M}|\Delta \boldsymbol{u}|\Delta t < d_\tau \longrightarrow \Delta t_{\max 3} = \dfrac{d_\tau}{M|\Delta u_{\max}|}$ $\qquad$ $\mathrm{M}|\Delta \boldsymbol{u}|\Delta t < 0.03 d_1 \longrightarrow \Delta t_{\max 4} = \dfrac{0.03 d_{1,\max}}{M|\Delta u_{\max}|}$

✓ Optimal operation : Δt = min ($\Delta t_{\max 1}, \Delta t_{\max 2}, \Delta t_{\max 3}, \Delta t_{\max 4}$) and $d_1 = d_{1,\max}$ with $d_{1,\min} < d_{1,\max}$

Experimental condition	Δt	Exposure	Flowrate including DEHS aerosol
Re=1500 (0.69m/s, 99LPM)	700μs	300μs	16LPM
Re=3000 (1.37m/s, 198LPM)	300μs	200μs	18LPM
Re=4500 (2.06m/s, 296LPM)	200μs	150μs	20LPM
Re=6000 (2.74m/s, 395LPM)	150μs	130μs	22LPM
Re=7500 (3.43m/s, 494LPM)	100μs	99μs	24LPM

Camera setting according to experimental conditions

✓ Near-wall region : $|\Delta u_{\max}|$ cannot be negligible in this experiment.

Experimental conditions

Experimental cases

Case no.	Inlet Re	T_{out} - T_{in}	Heat removal	U_b (x = 1.4 m)	Re_b (x = 1.4 m)	Flow regime
1	7700	0 K	-	3.40 m/s	7700	Turbulent
2	5500	0 K	-	2.43 m/s	5500	
3	2000	0 K	-	0.88 m/s	2000	Laminar
4	7700	29.2 K	293 W	3.64 m/s	7320	Turbulent forced
5	5500	32.7 K	234 W	2.62 m/s	5200	
6	7700	64.7 K	653 W	3.92 m/s	6920	
7	5500	70.4 K	508 W	2.84 m/s	4910	↕
8	5500	79.0 K	572 W	2.89 m/s	4850	
9	5000	81.5 K	536 W	2.64 m/s	4390	
10	4500	88.0 K	521 W	2.41 m/s	3910	Turbulent mixed
11	4200	88.2 K	488 W	2.25 m/s	3500	

Measurement locations (x = 1.4 m)

- To capture the near-wall flow characteristics and behaviors of corner flows
  - 'Wide' direction: y = -6 mm, 0 mm, 6 mm, 'Narrow' direction: z = 0 mm, 45 mm, 56 mm

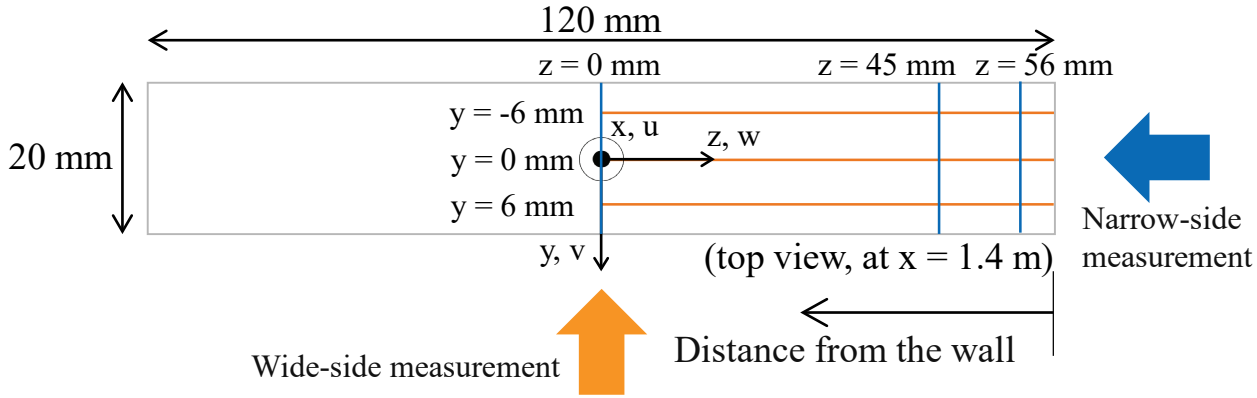

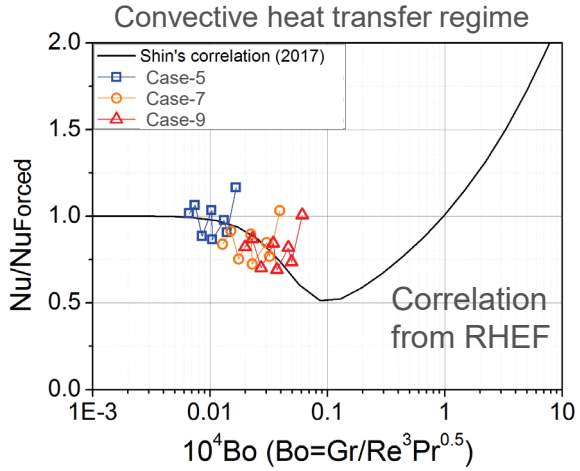

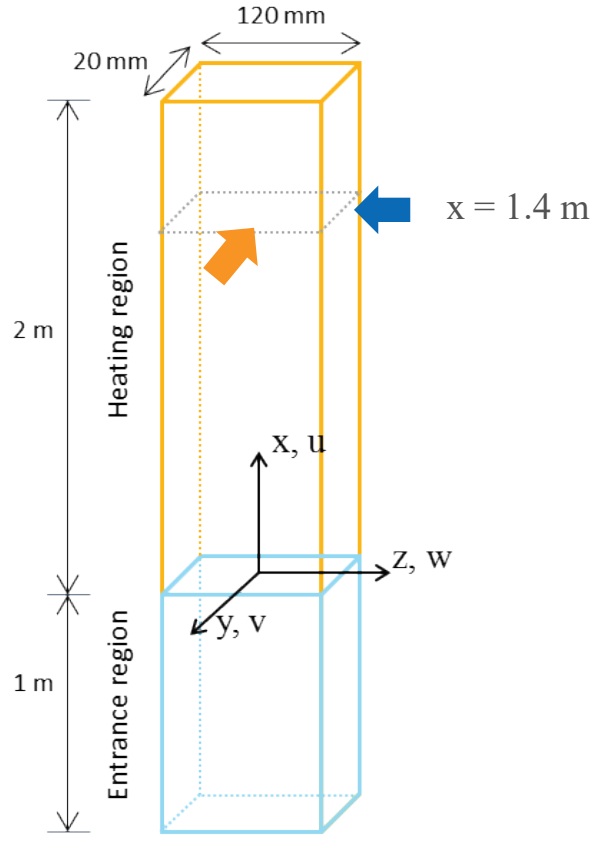

Test section and coordinate system

Validations for experimental data

Uncertainty analysis

- Time averaged measurement variables (60 s → 1500 velocity vector fields)
  - Precision error; five times repeated → t-distribution
- The bias error due to the PIV equipment; about 1% of the average velocity.
  - Bias errors from other measurement instruments were considered.

- PIV equipment uncertainty parameters

Parameter	Description	y_i	w_i
l	Calibration scale physical length	20 mm	0.2 mm
L	Calibration scale image plane length	800 pixels	1 pixel
λ	Distance from calibration scale to lens	1 m	0.5 mm
t	Laser pulse timing	100 μs	20 ns

- Uncertainties of the measured variables

Parameter	Instrument	Uncertainty
Flow rate	Thermal mass flowmeter	0.48%
	Variable-area meter	12.5 cm^3/s
Temperature	K-type thermocouple	1.1 ℃
Power	Variable switching power supply	0.60%
Pressure	Pressure transmitter	2 mbar

Validations for turbulence quantities

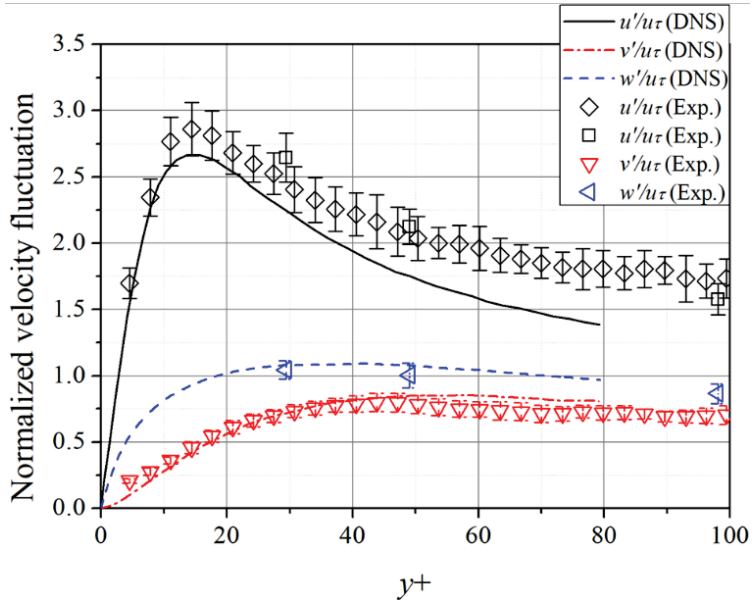

RMS velocity fluctuation distributions
(lines: DNS, Kim et al. (1987), symbols: experimental data)

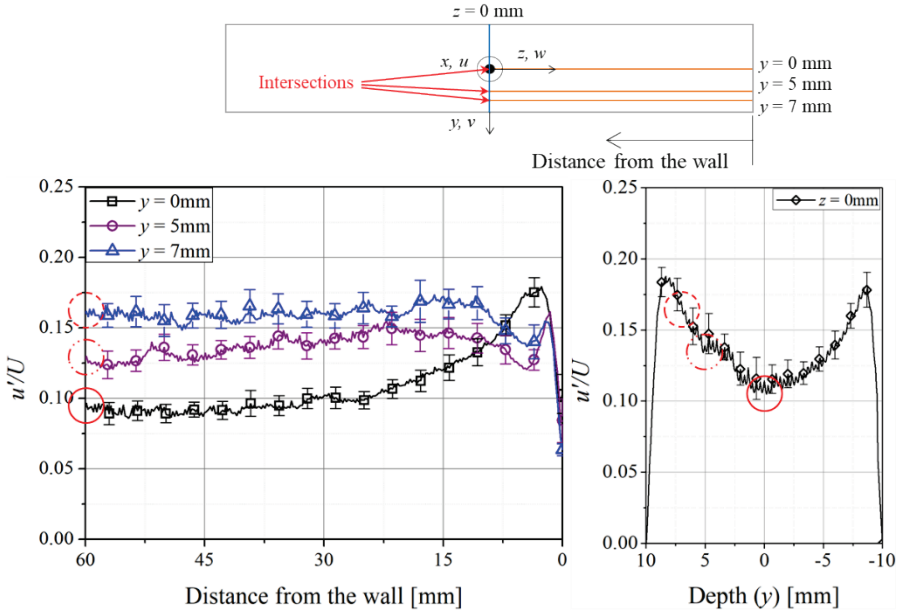

Vertical velocity fluctuation matching

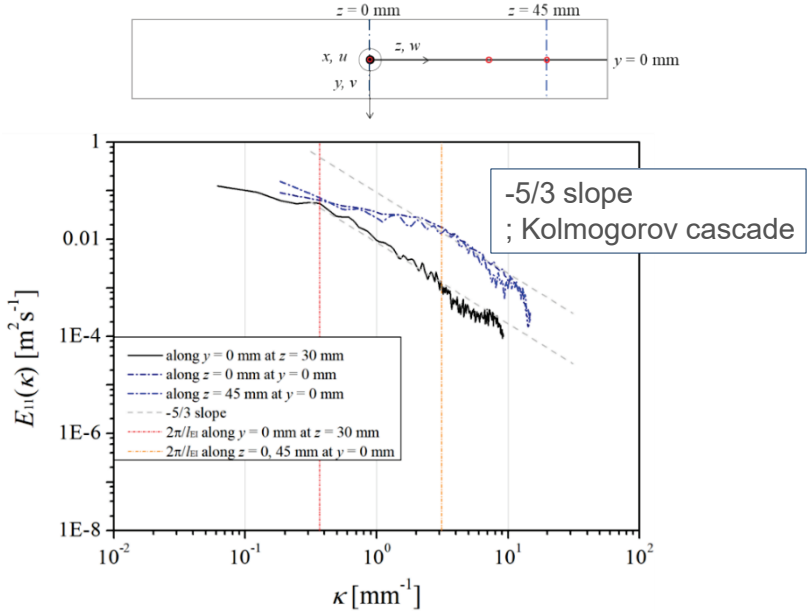

Energy spectrum analysis

Results of the experiment

Overall velocity distribution nondimensionalized by the bulk velocity

- ✓ Flow laminarization in mixed convection (→ Heat transfer deterioration)

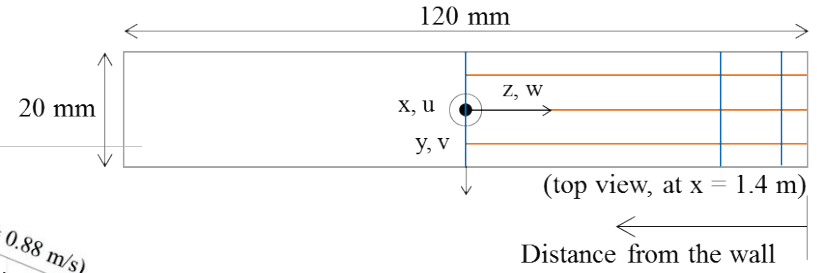

Non-heating conditions;

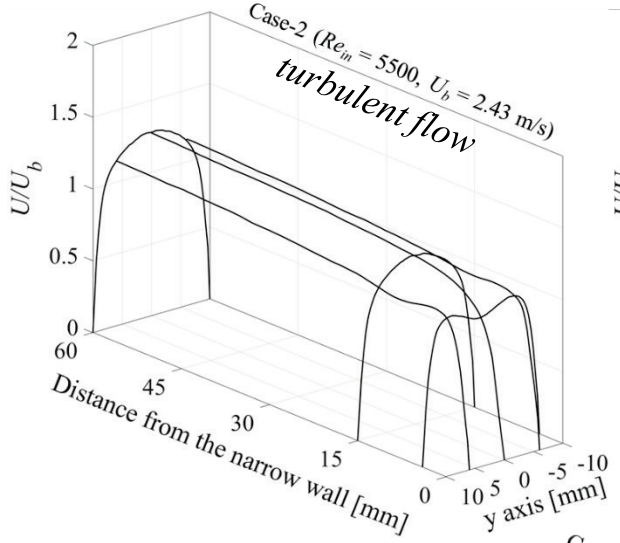

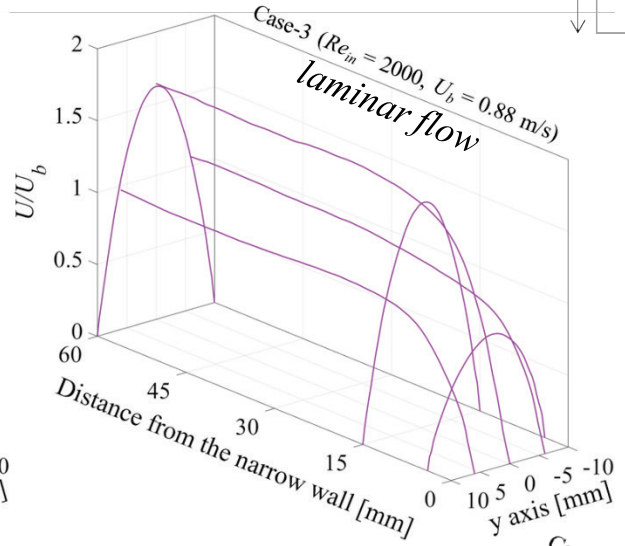

Heating conditions;

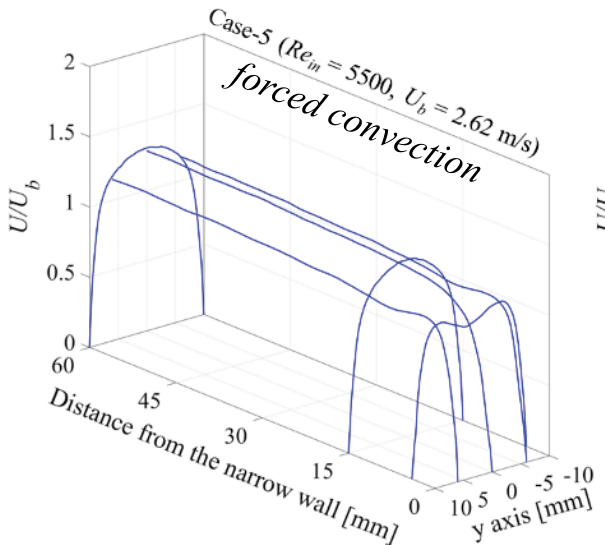

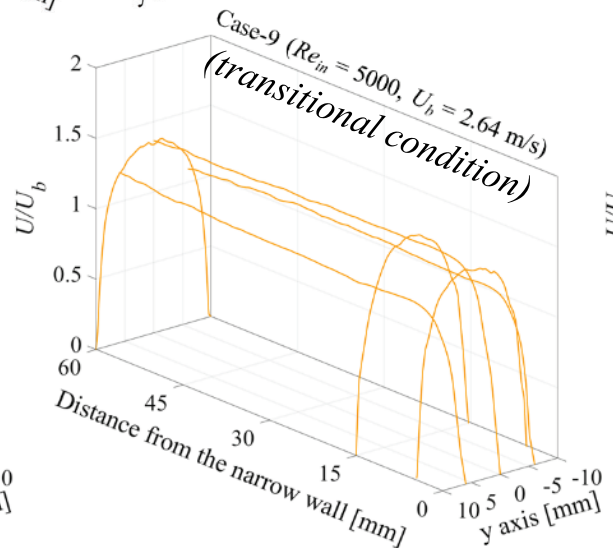

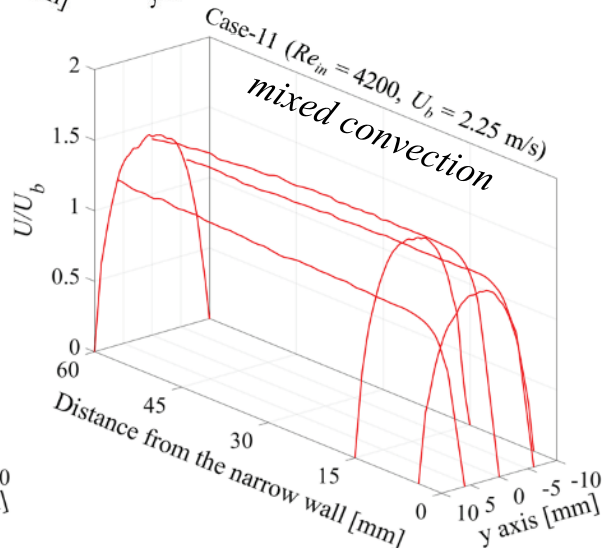

Results of the experiment

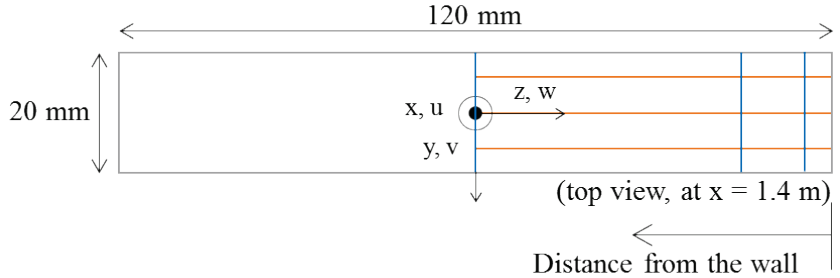

Reynolds shear stress

– Primary Reynolds shear stresses ($\overline{u'w'}$ and $\overline{u'v'}$) including primary velocity fluctuation u'

✓ Flow laminarization preceding near the corners

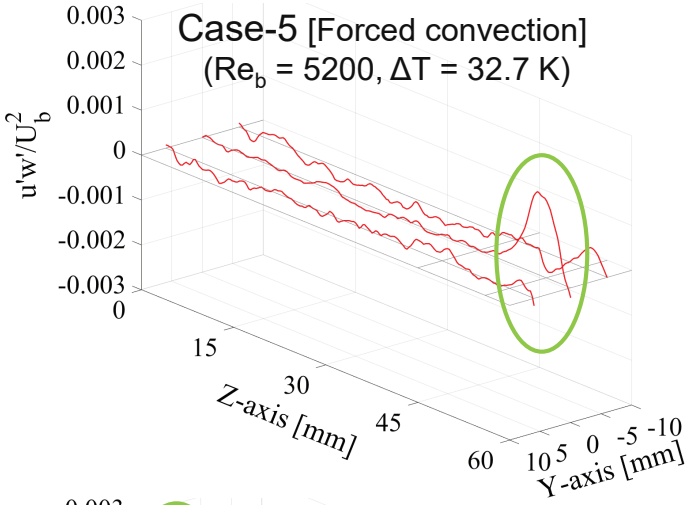

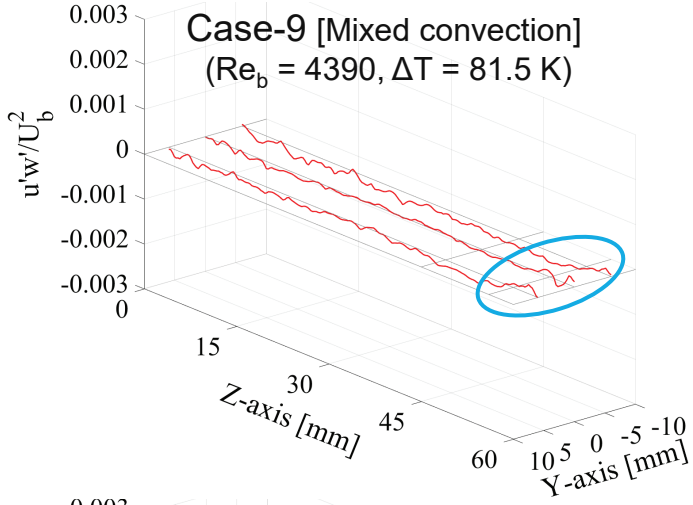

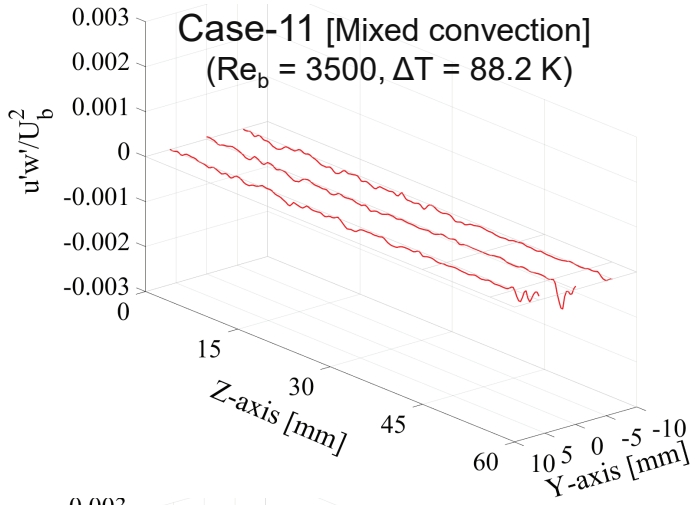

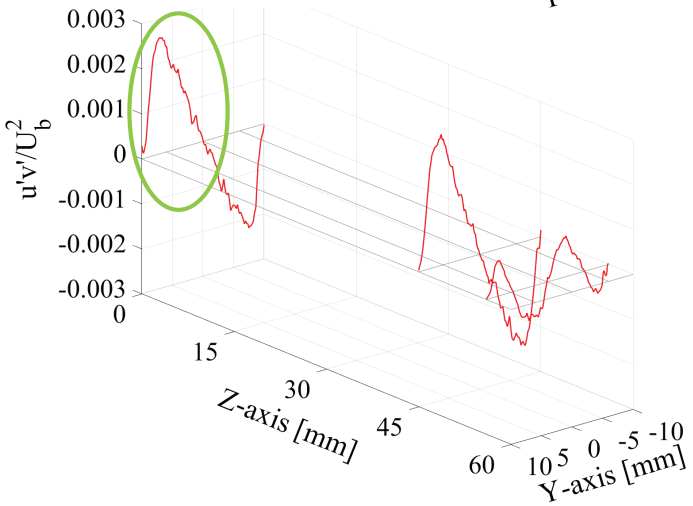

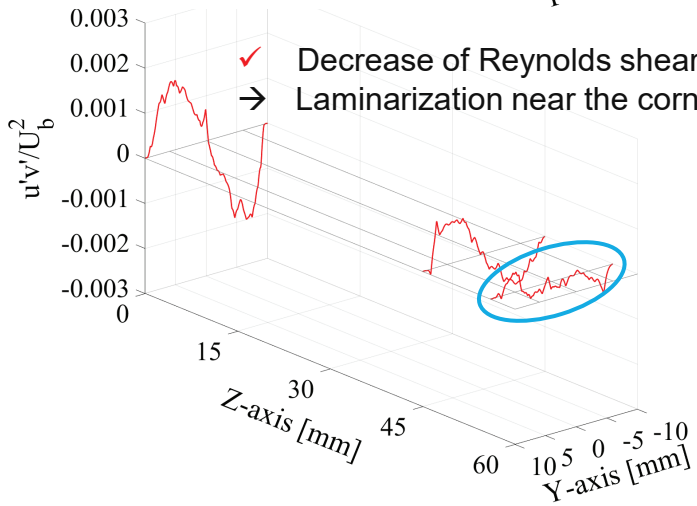

✓ Decrease of Reynolds shear stress
→ Laminarization near the corner first

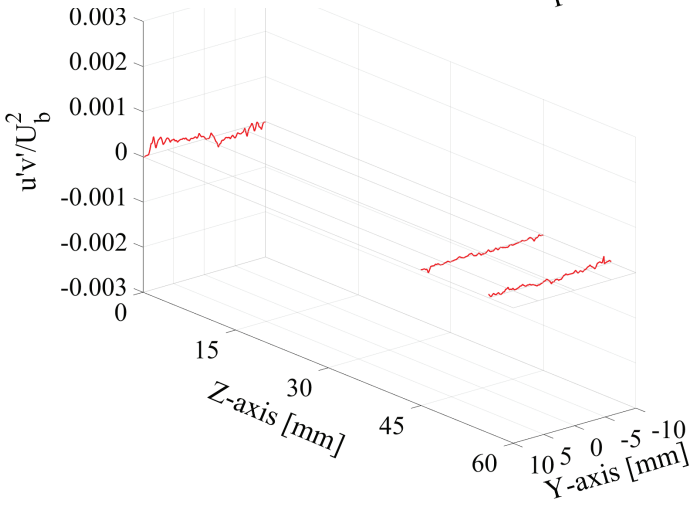

Temperature measurement

Local temperature distribution of airflow

- FBG sensor (Fiber Bragg Grating sensor)
  - 10 mm-average value (0.2 mm diameter)
- ✓ Response time → Temperature fluctuation

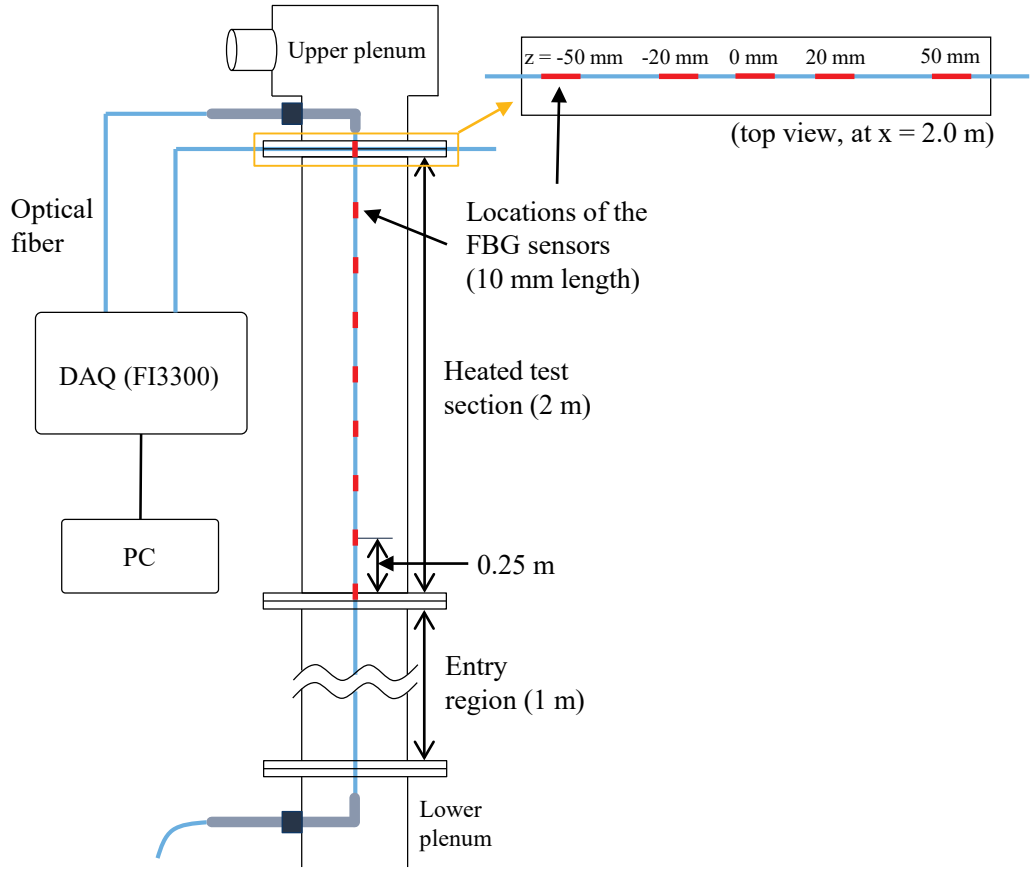

Schematics of the local temperature measurement system using FBG sensor

Outer wall temperature distribution of the test section

- Infrared thermometry
  - For the temperature boundary conditions in CFD analyses
- Heat transfer quantification
  - Heat losses through the test section cannot be controlled or measured.
- Emissivity calibration: ε = 0.93
  - By comparing the wall temperature
    ; Infrared camera ↔ self-adhesive thermocouples

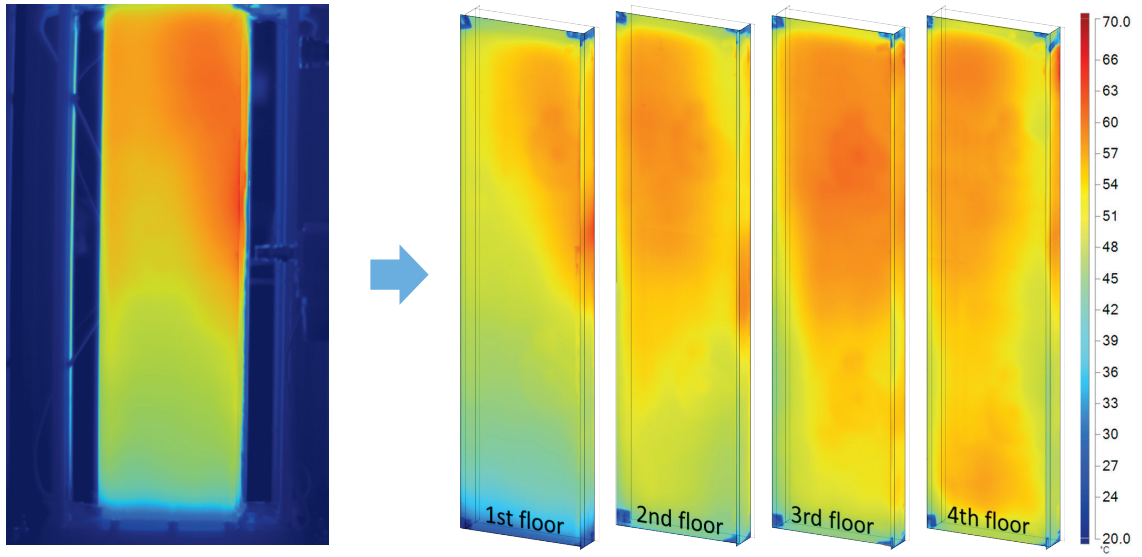

Captured outer wall temperature distribution by infrared camera

CONTENTS

CFD analysis: Development of turbulence modeling

7 turbulence models (EVMs) in STAR-CCM+

- STAR-CCM+ User guide

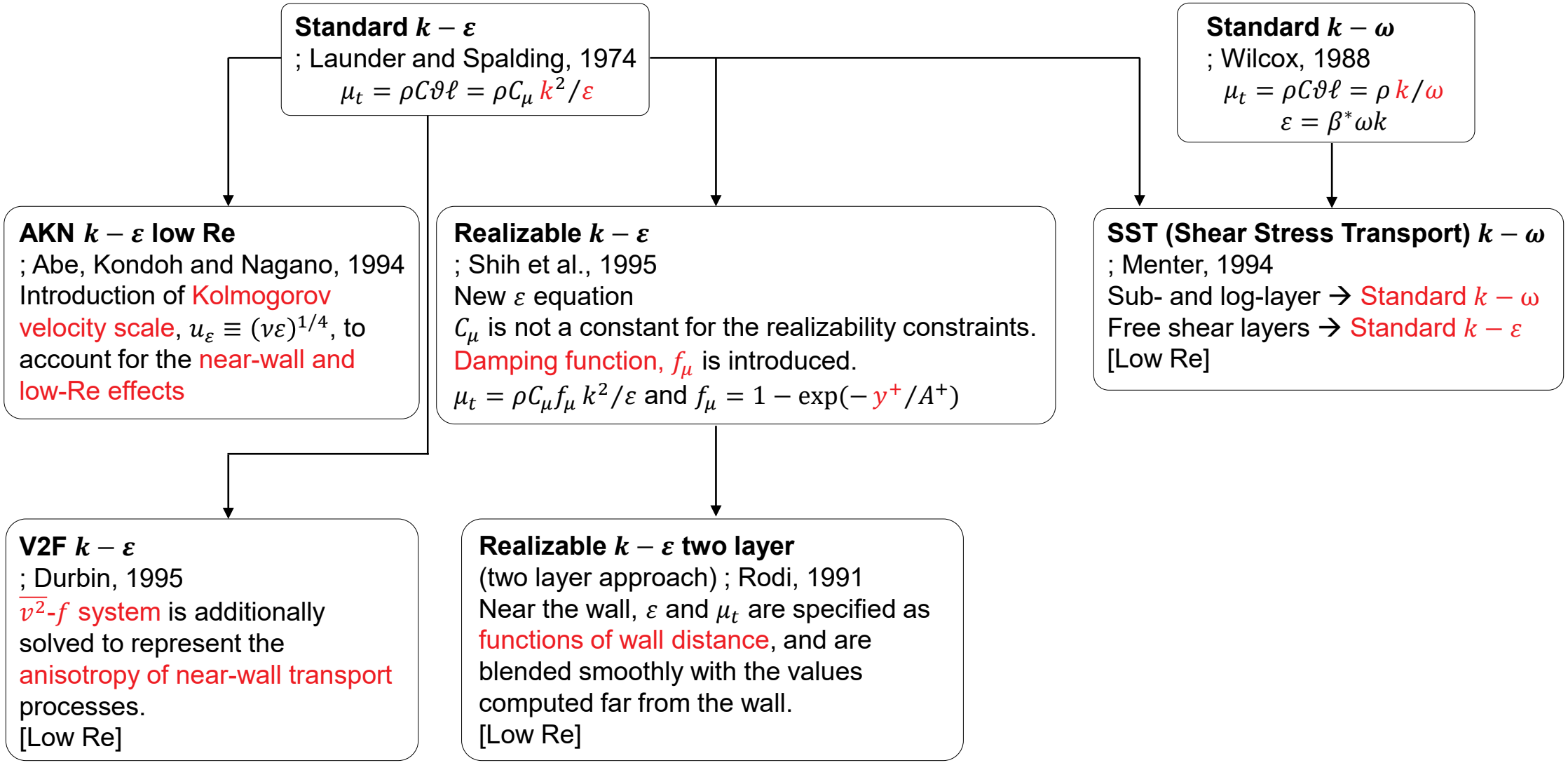

Calculation conditions

STAR-CCM+ 13.02

✓ Calculation geometry

- Rectangular channel
  - Channel: 120 mm x 20 mm x 2000 mm (W x D x H)
- Solid part with conjugate heat transfer (to consider conduction effect)
  - 1 μm-thickness FTO coating, 4 mm-thickness heat-resistant glass

✓ Boundary conditions

- Outer wall temperature boundary conditions (IR thermometry)
- Volumetric heat sources; applied power in the experiment
- Distributions of developed velocity and **turbulence quantities at inlet**

$$k;\ \frac{3}{2}(IU_{in})^2,\ \varepsilon;\ \frac{C_\mu^{3/4}k^{3/2}}{L}$$

$$I = 0.16\mathrm{Re}^{-1/8},\ L = 0.07D_h$$

In experiment!

Mesh generation

- Grid sensitivity test (V2F *k-ε* model)
- Mesh models
  - About 5.2 million cells (Axial: 700 cells)
  - Hexahedral cells, surface remesher, prism layer mesher (5 layers with 1.5 stretching for 0.7 mm)

Physical models (Steady)

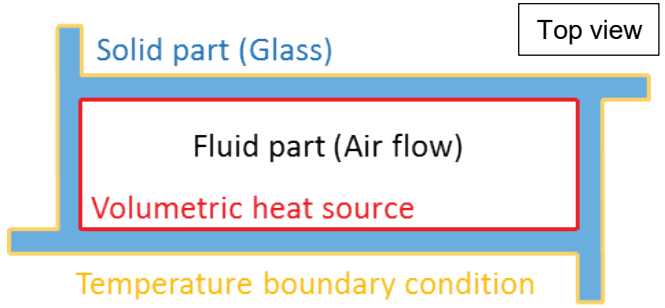

Concept of CFD calculation geometry and boundary conditions for turbulence model assessment

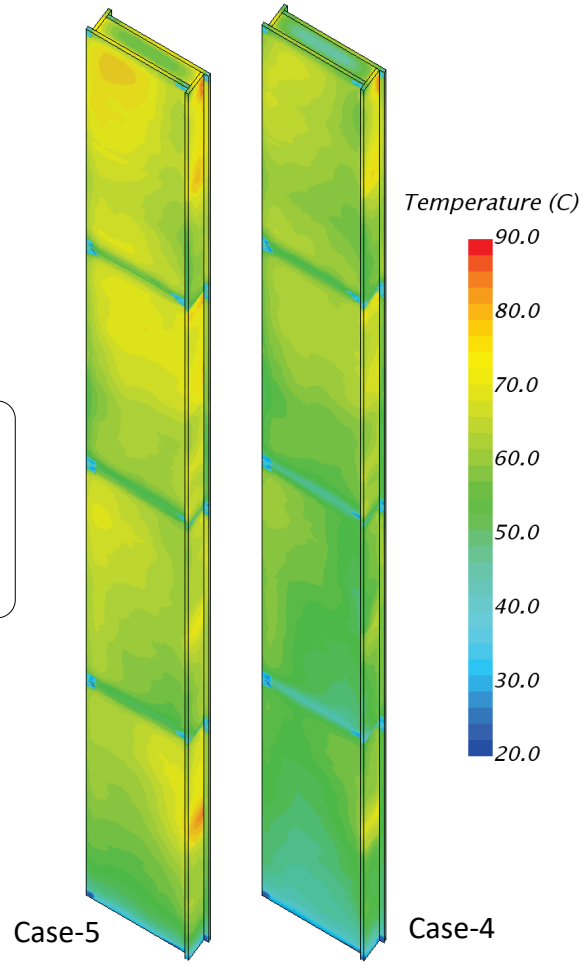

Temperature distribution imposed in the CFD calculation

Results of CFD analysis

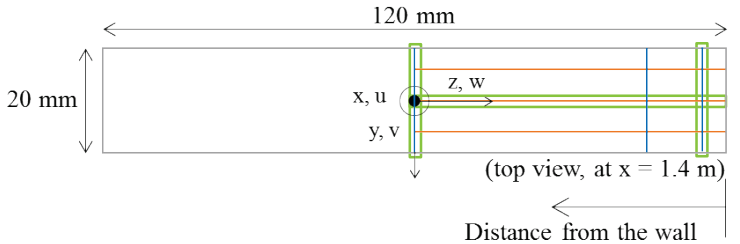

Local flow structure with experimental data

- Vertical velocity was underestimated by the models near the corner.
- Laminarization near the corner can not be predicted by CFD analysis → Higher heat transfer rate by CFD

➢ *Case-2 (Re=5500, ΔT=0K)*

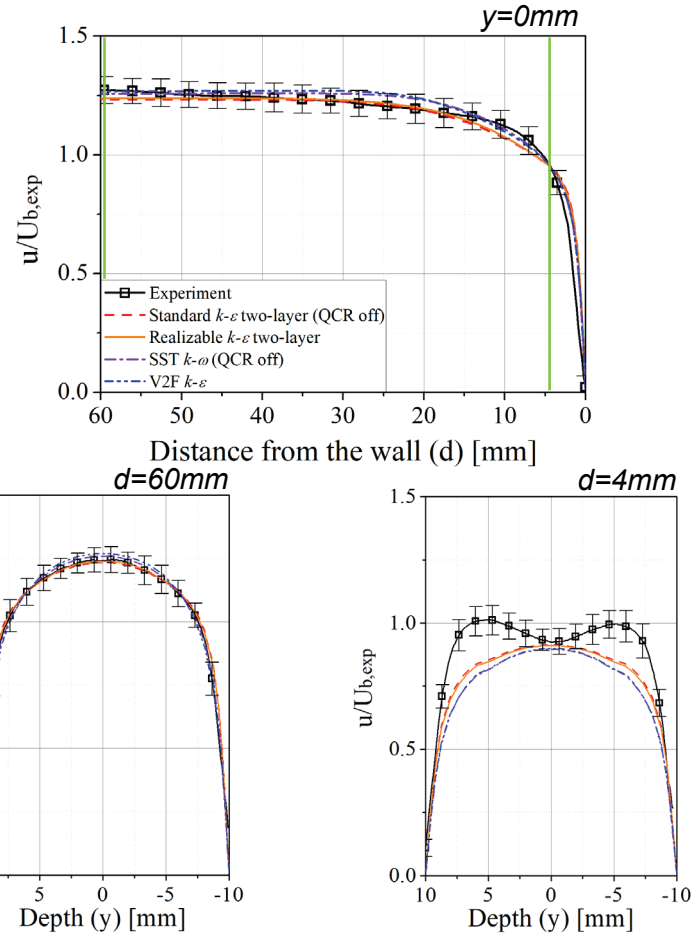

➢ *Case-9 (Re=5000, Re_b=4400, ΔT=81.5K)*

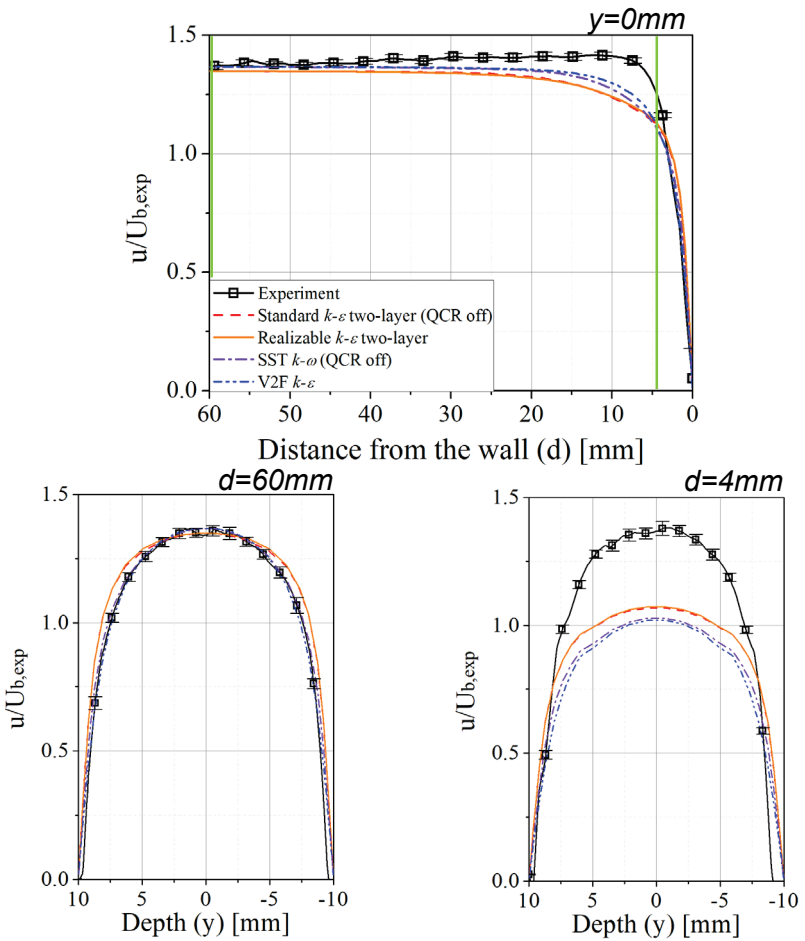

Results of CFD analysis

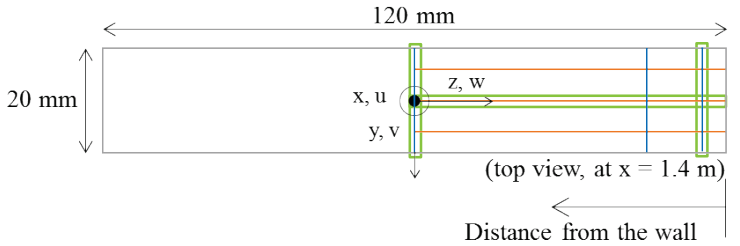

Reynolds shear stress with experimental data

- Turbulence models overpredict Reynolds shear stress distribution.
- In mixed convection conditions, Reynold shear stress ∝ heat transfer

➢ *Case-2 (Re=5500, ΔT=0K)*

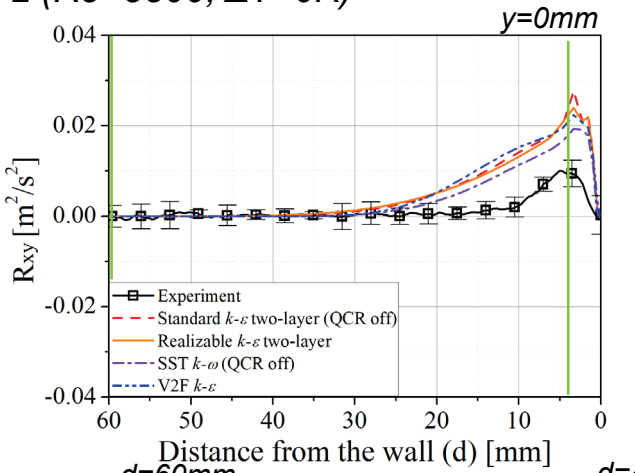

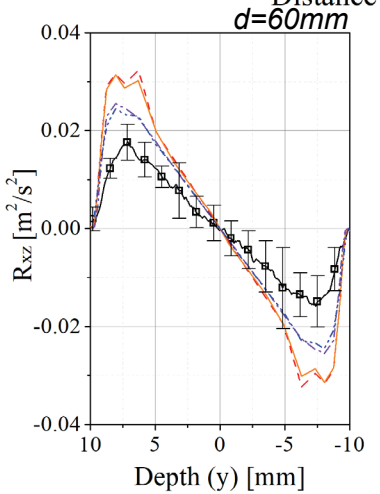

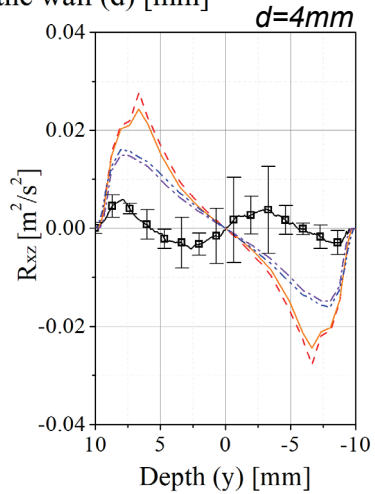

➢ *Case-9 (Re=5000, Re_b=4400, ΔT=81.5K)*

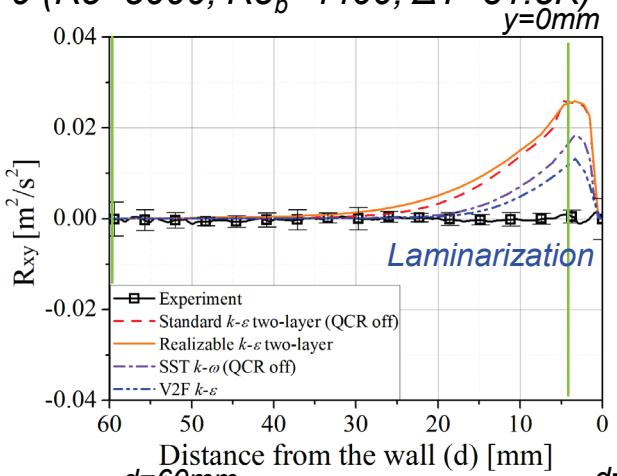

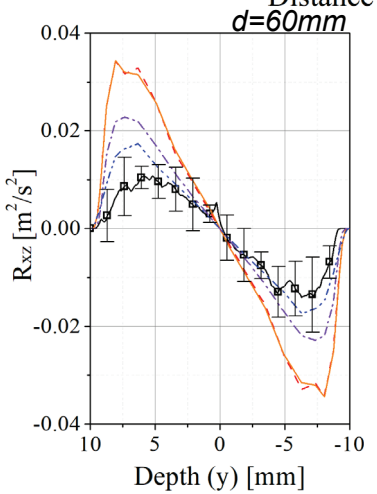

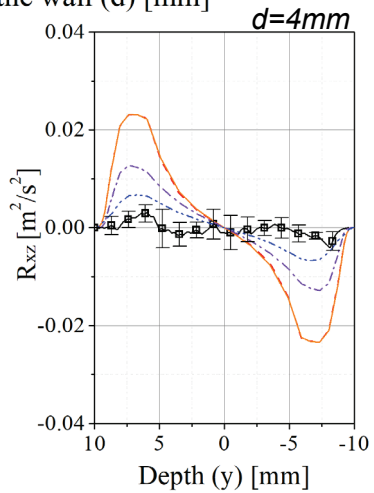

$$* R_{ij} = \nu_T \left(\frac{\partial \langle U_i \rangle}{\partial x_j} + \frac{\partial \langle U_j \rangle}{\partial x_i} \right)$$

✓ V2F ***k-ε*** model can predict the decrease of Reynolds shear stress.

Results of CFD analysis

Inlet/outlet temperature difference

✓ V2F k-ε model
; lowest heat transfer prediction, closest to experimental results

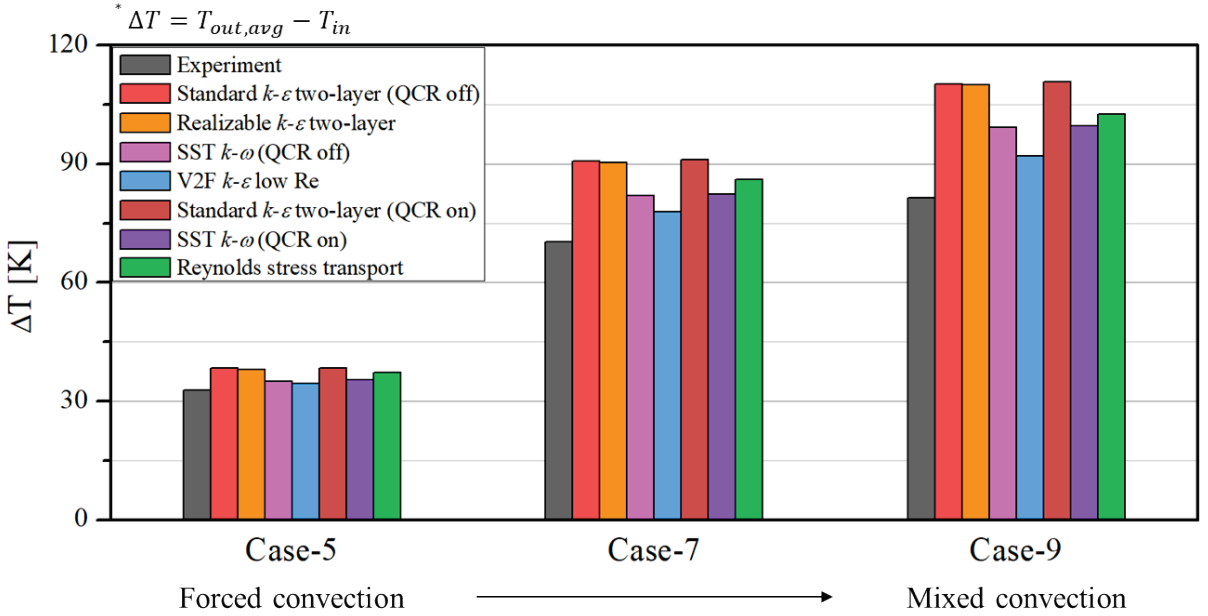

Riser heat transfer quantification

- Heat transfer coefficient; $h = q''/(T_s - T_b)$ (From CFD)
- Visualization experiment: heat loss control is impossible.
  → Non-uniform heat flux along the elevation
- Heat flux along the elevation : Results from V2F model

$$q''_{Esti.} = q''_{V2F} \times \frac{(T_{out} - T_{in})_{Exp}}{(T_{out} - T_{in})_{V2F}}$$

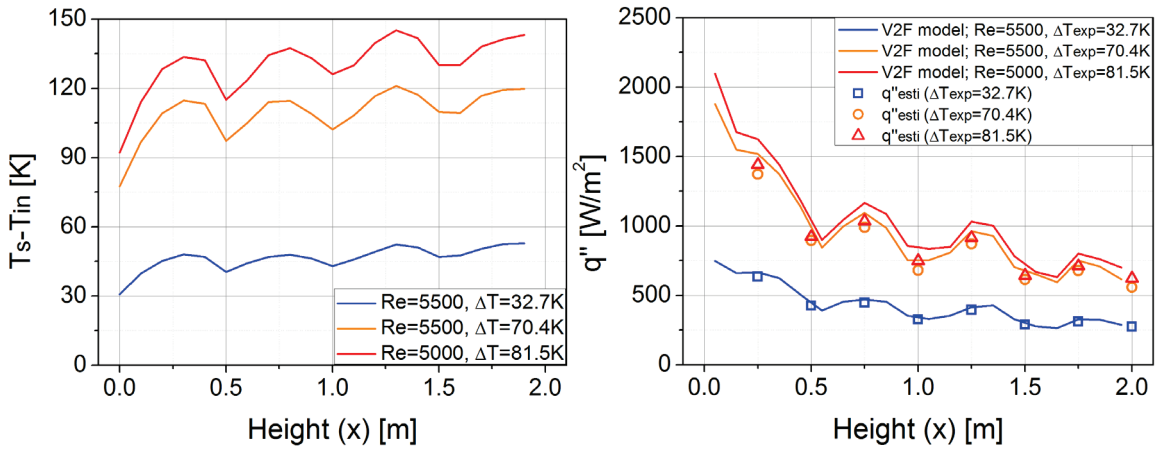

Inner wall T distribution (left) and heat flux distribution (right) along the elevation

✓ Nusselt number, $Nu = hL/k$

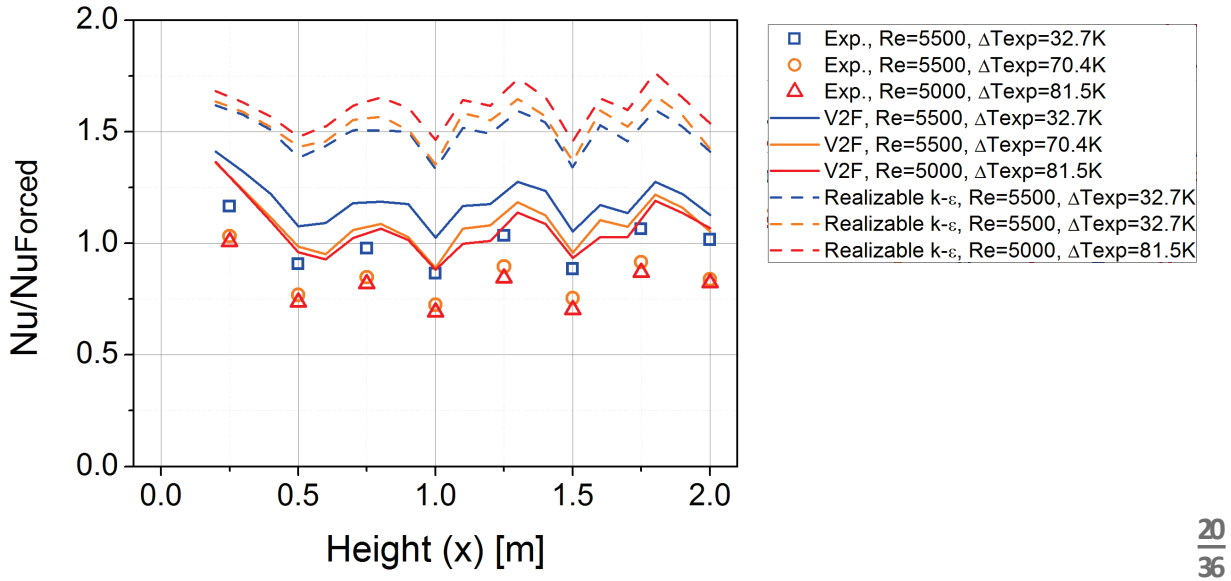

Results and discussions

Heat transfer coefficient

- ✓ The models overestimated the heat transfer coefficient compared to that of the experiment.

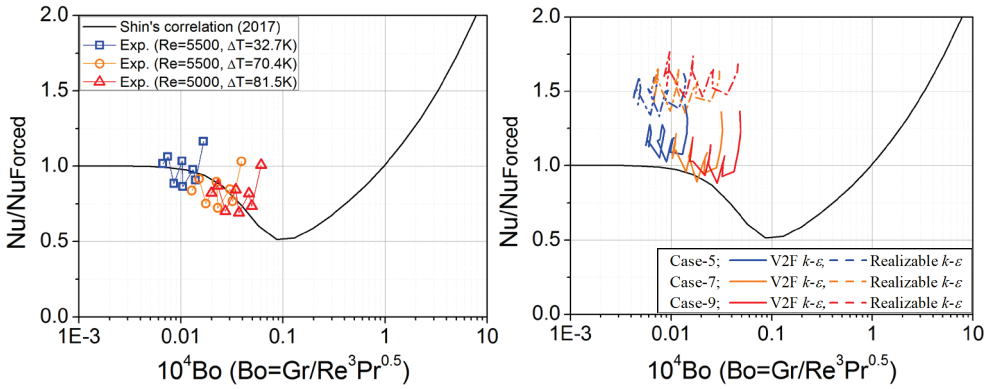

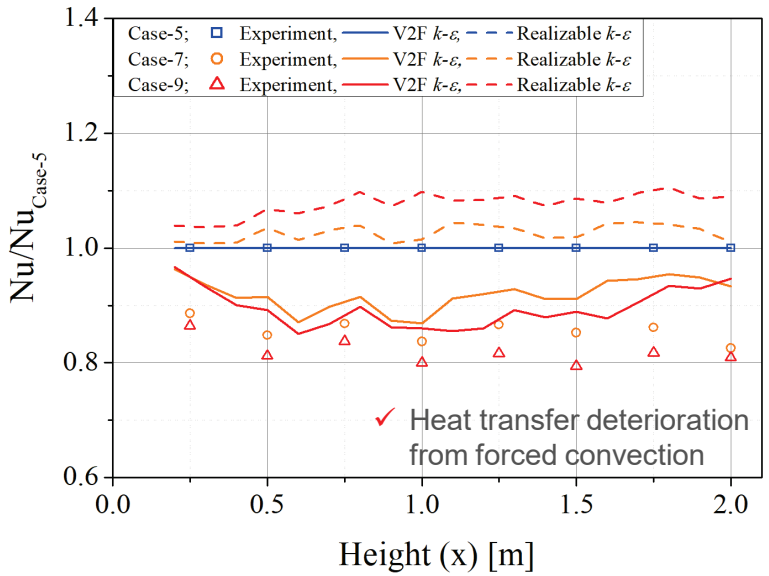

Transition from forced to mixed convection

- ✓ Normalized temperature distribution is not changed by the turbulence models.

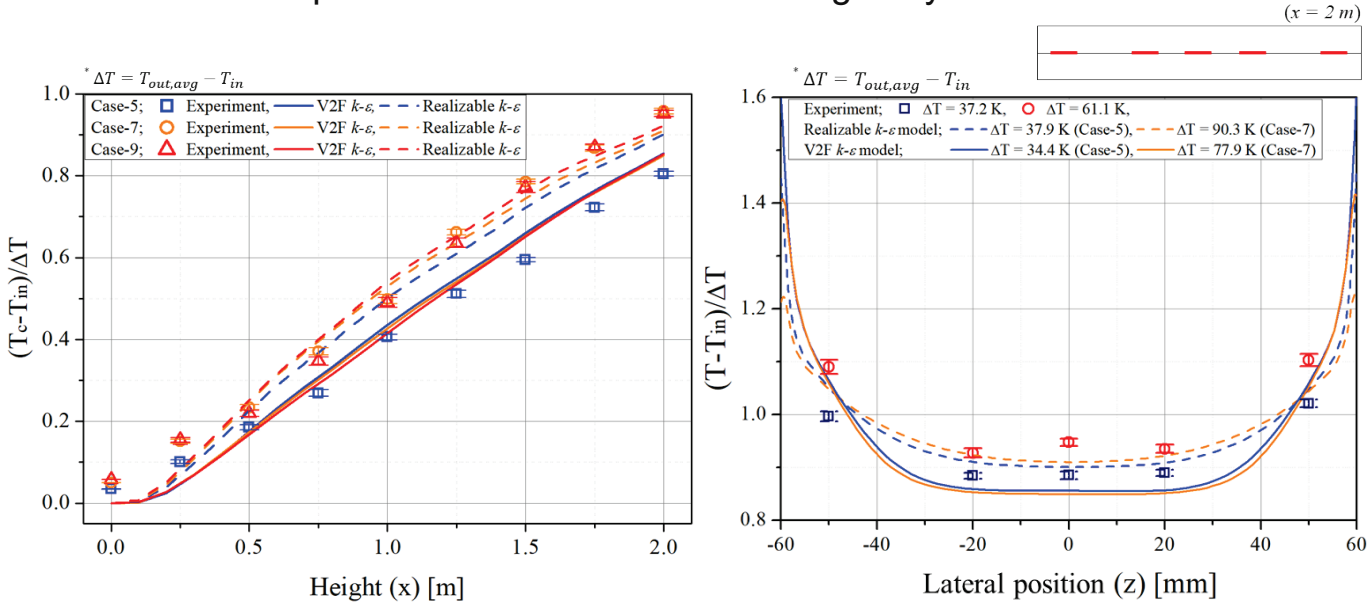

The local temperature distribution normalized by the each inlet/outlet temperature difference in the experiment and CFD analysis ; along the centerline (left) and at the outlet (right) of the test section

- ✓ Laminarization preceding near the corner was also not predicted.

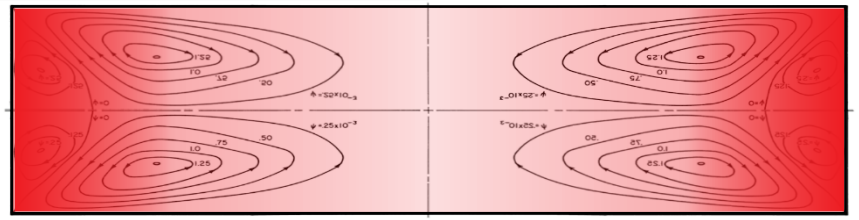

Transition of the heat transfer phenomena in a rectangular channel

CONTENTS

Wall-bounded turbulence

Vortex

— The flow revolves around an axis line in this region.

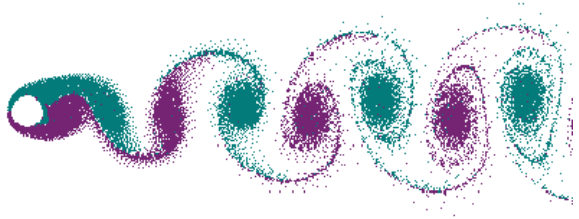

• Karman vortex street
; a repeating pattern of swirling vortices

Turbulence

— Vortices of many sizes appear and interact with each other.

— Kinetic energy → Turbulent stresses

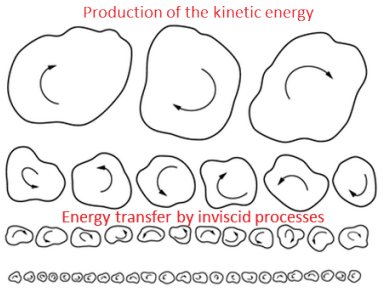

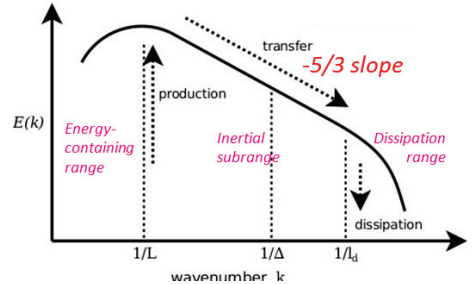

Formation of Reynolds shear stress

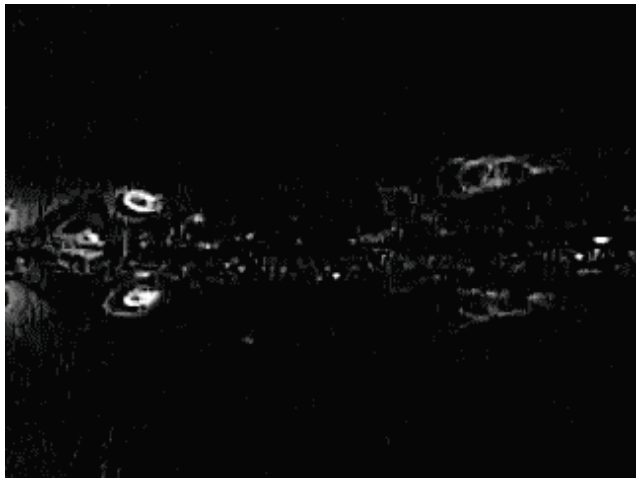

Flow visualization of a laminar hairpin vortices

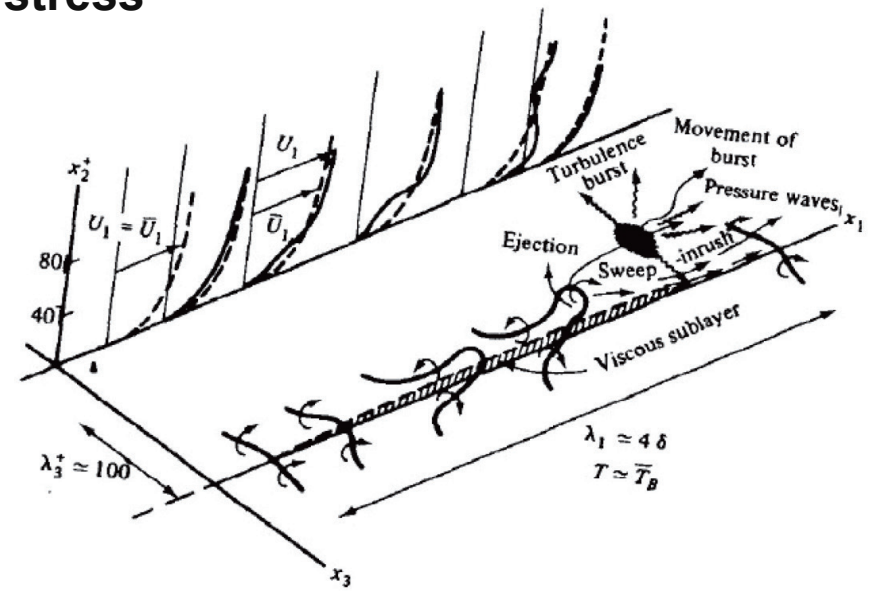

Figure 14 - Conceptual model of the turbulence near the wall during a "cyclic" process (from Hinze 1979)

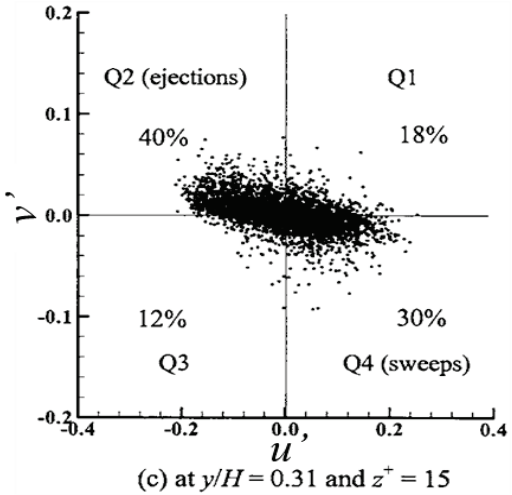

(c) at $y/H = 0.31$ and $z^+ = 15$

Instantaneous velocity fluctuation data [Joung et al., 2007]

Reynolds shear stress

Mixed convection heat transfer

– Explanation for the heat transfer deterioration and enhancement
; Changes in Reynolds shear stress distributions

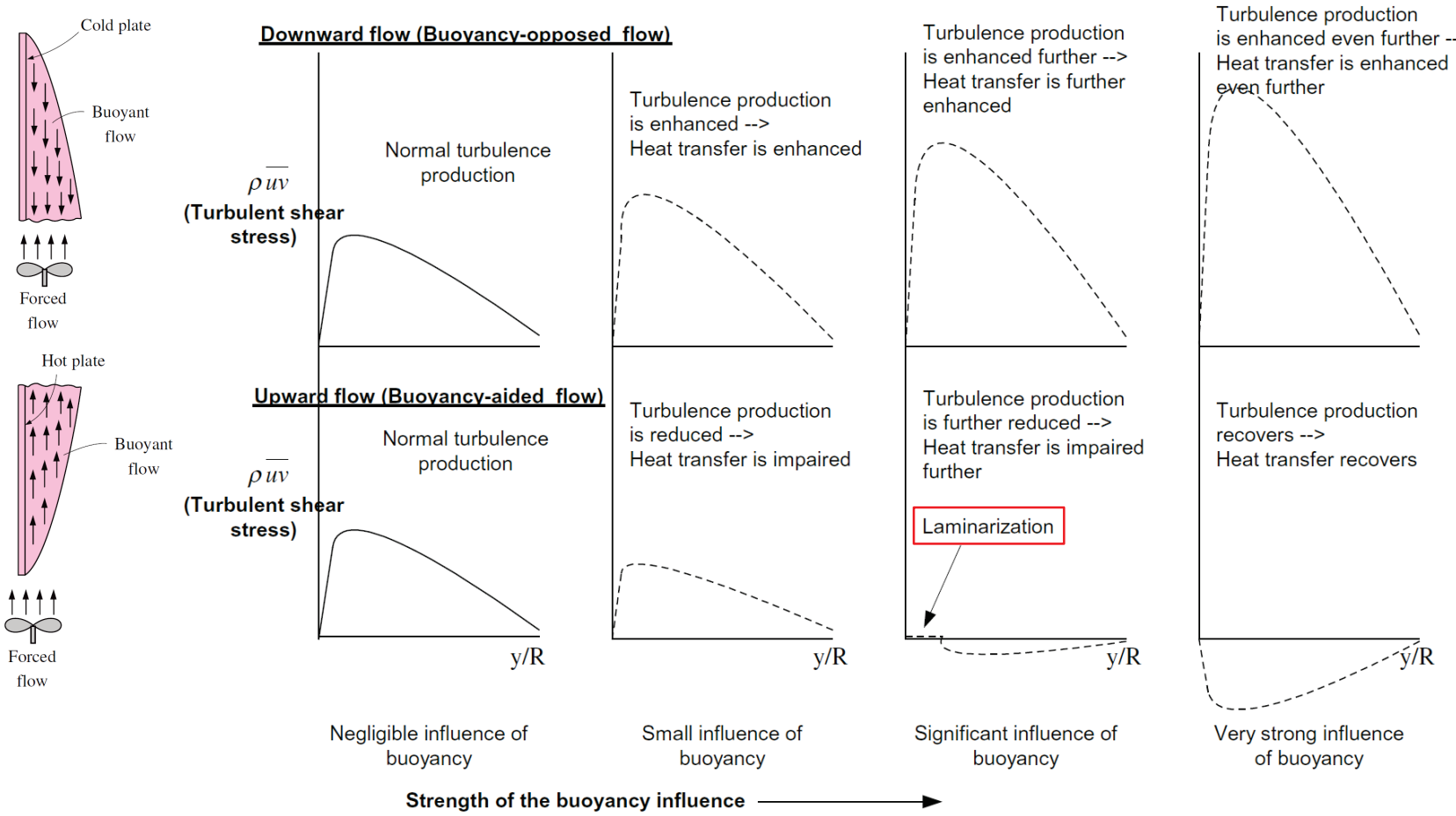

Reynolds shear stress for buoyancy-opposed and buoyancy-aided flow [Kim et al., 2008]

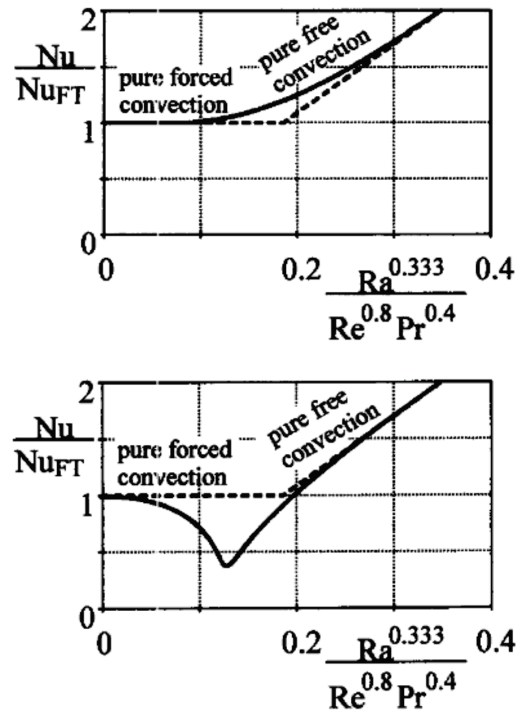

Schematic diagram showing heat transfer for opposing (up) and aiding (down) mixed convection [Aicher and Martin, 1997]

Discussion 1. Heating effect near the wall

Quadrant analysis with linear correlation (slope)

- ✓ Cause of Reynolds shear stress decrease in the mixed convection
  1) Decrease of wall-bounded vortex motion?
  2) Occurrence of another vortex motion?
- ✓ In natural convection with intense heating, $\overline{u'v'} > 0$.

Therefore, heating induces vortex motion independent of the wall-bounded vortex.

Pearson's correlation coefficient; $\rho_{u\prime,v\prime} = \frac{\mathrm{cov}(u\prime,v\prime)}{\sigma_{u\prime}\cdot\sigma_{v\prime}} = \frac{\overline{u'v'}}{\sqrt{\overline{u'^2}}\sqrt{\overline{v'^2}}} = \frac{R_{xy}}{\sqrt{R_{xx}R_{yy}}}$

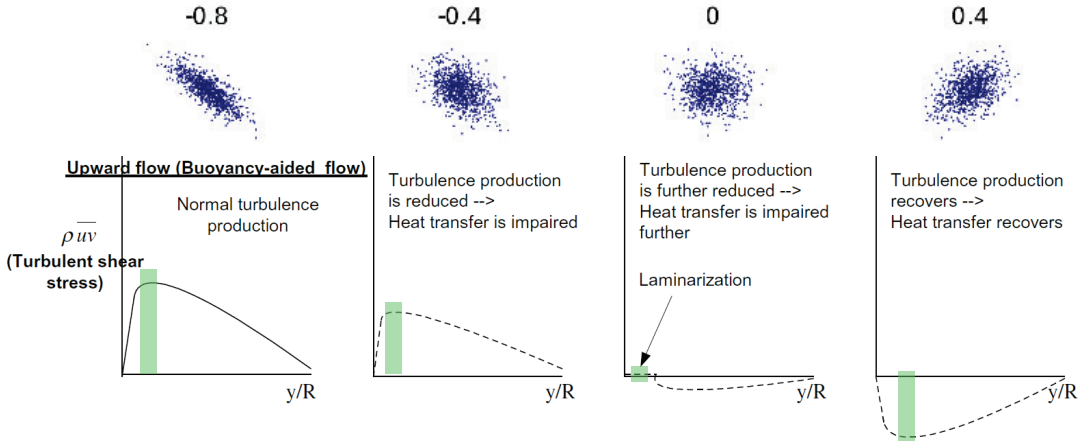

Examples of scatter diagrams for the heat transfer deterioration in mixed convection

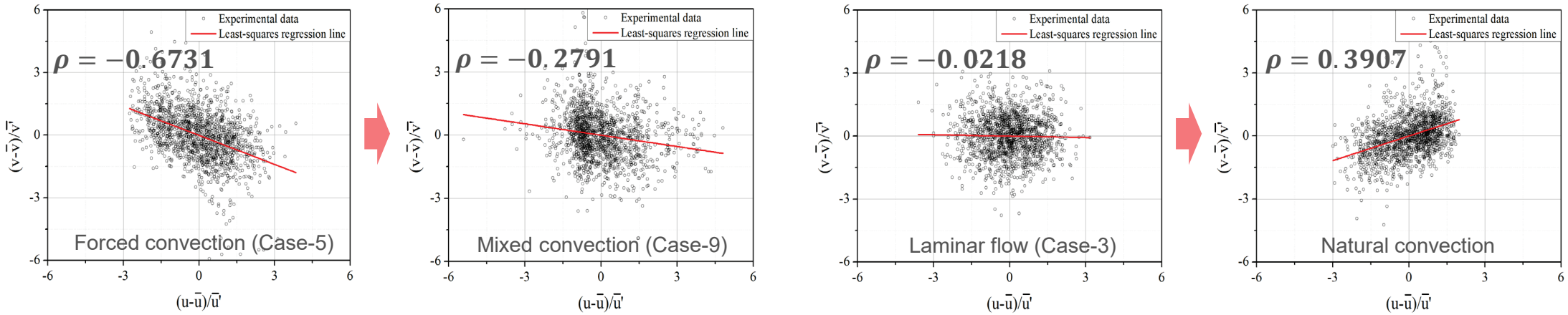

Quadrant analysis results

Discussion 1. Density-gradient induced vortex

Heating effect near the wall

— Temperature gradient along the wall-normal direction

✓ Large density gradient in the viscous sublayer → Another repetitive vortex motion independent of the wall-bounded vortex

Buoyancy-aided flow

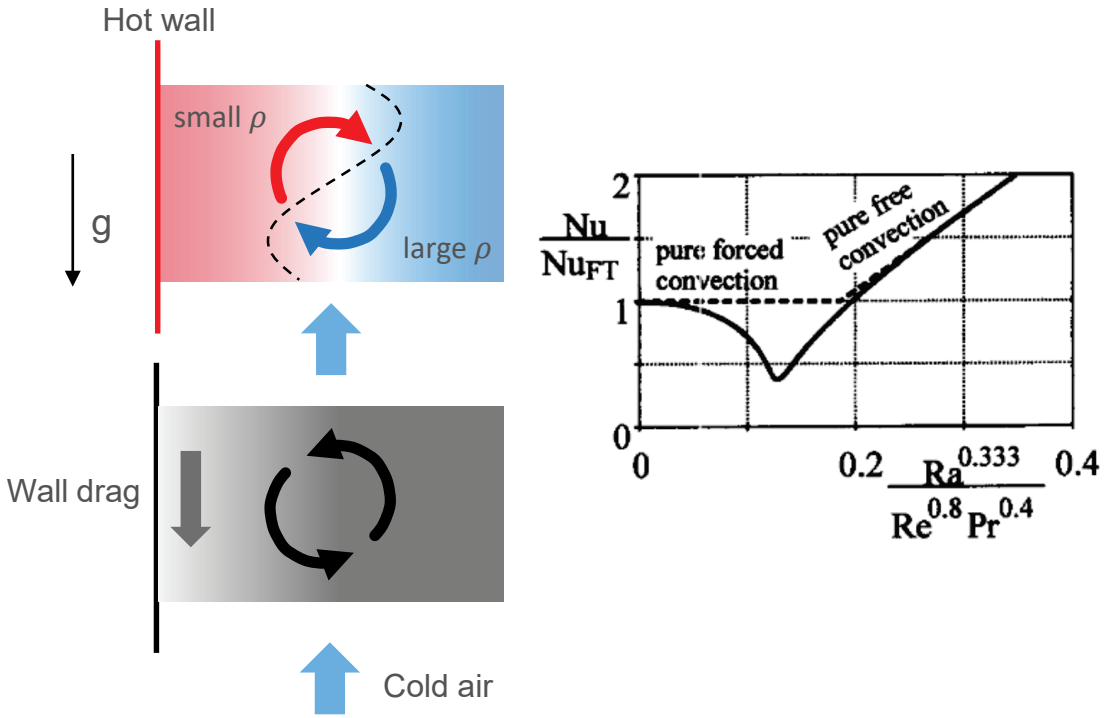

Buoyancy ∥ Flow ➔ Heat transfer deterioration with R_{xy} ↓

∵ Wall-bounded vortex ↔ Density-gradient induced vortex

Buoyancy-opposed flow

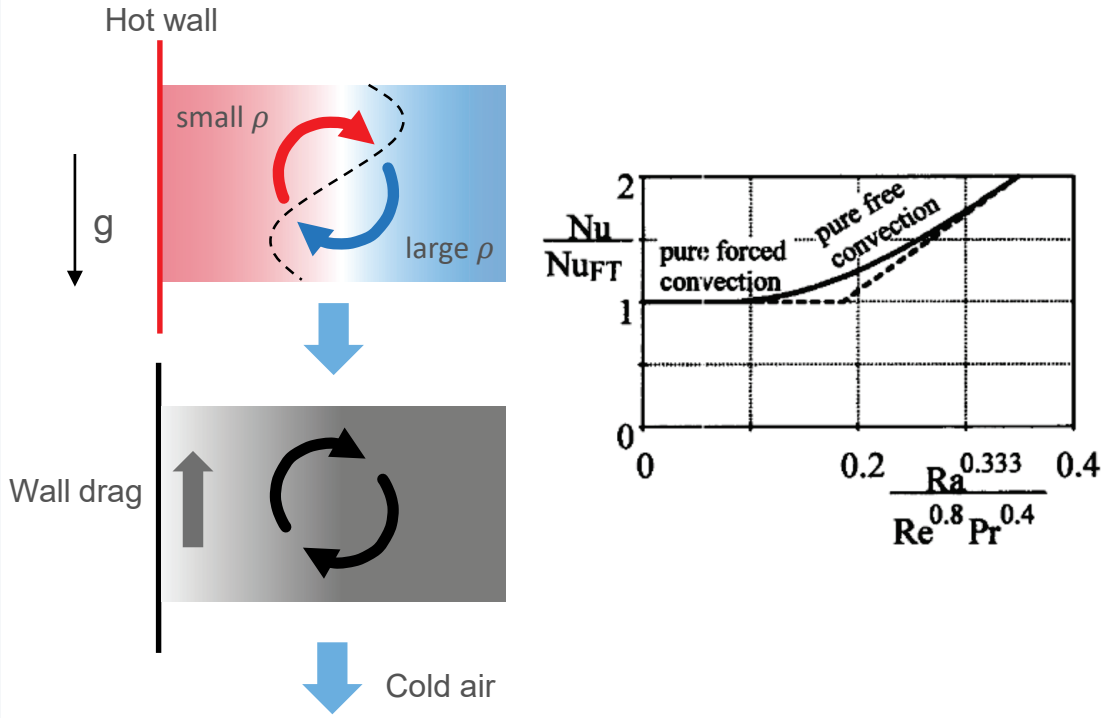

Buoyancy ↔ Flow ➔ Heat transfer enhancement with R_{xy} ↑

∵ Wall-bounded vortex ∥ Density-gradient induced vortex

Discussion 2. Flow characteristics along corner bisectors

Primary Reynolds shear stresses

— Complex and low distribution near the corners

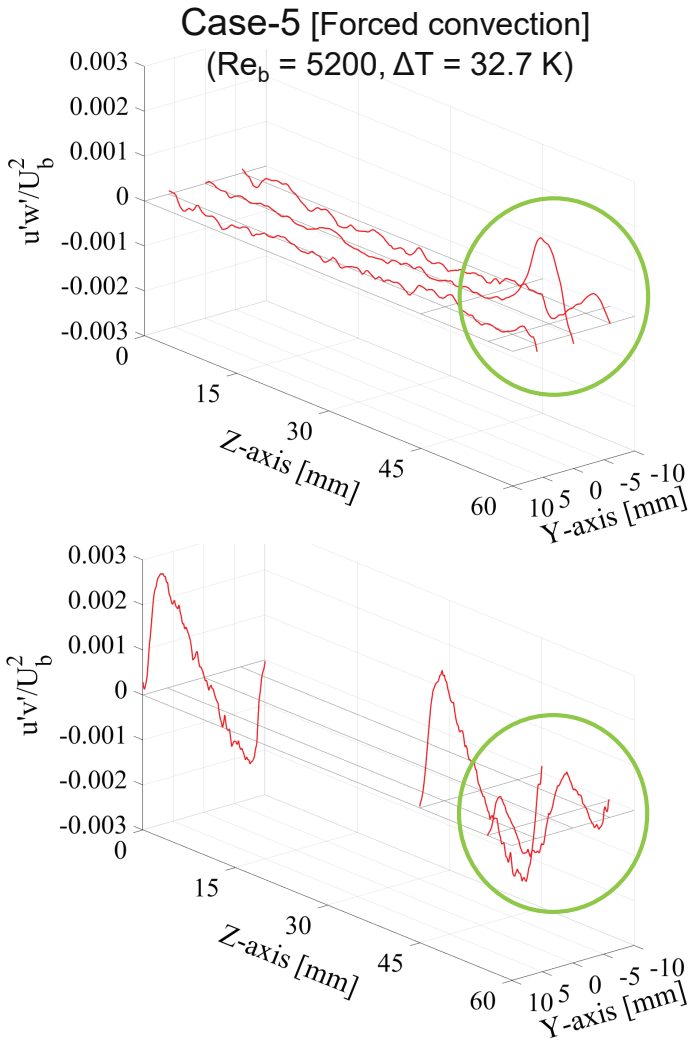

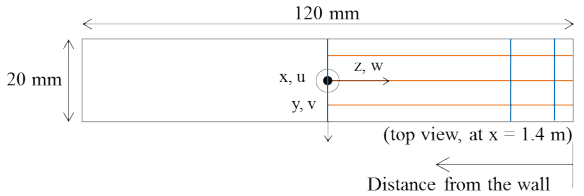

✓ Schematic diagrams for intuitive understanding of primary Reynolds shear stresses, $\overline{u'w'}$ and $\overline{u'v'}$

① The shear stress distribution is formed along the wall-normal direction.

② On the line of symmetry (corner bisector), they cancel each other formed from opposite (orthogonal) walls.

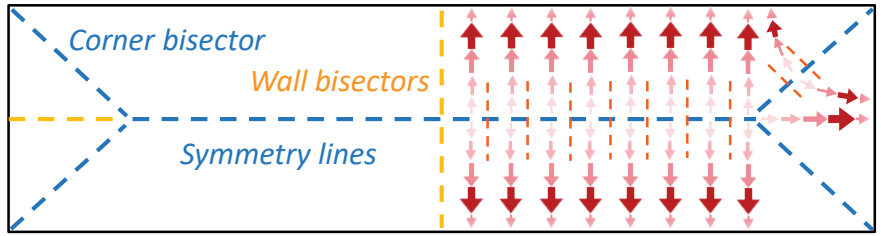

* top view

➢ It can be described with a newly defined vector; $\overline{u'v'}\hat{j} + \overline{u'w'}\hat{k}$

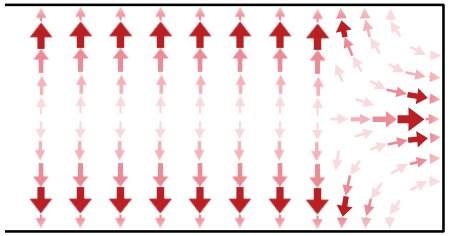

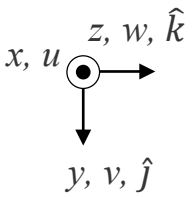

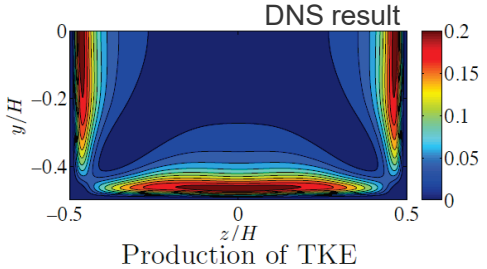

➢ Along the corner bisectors, the Reynolds shear stress is canceled in reality, rather than superposed.

✓ *Cancellation of the linear relationships from orthogonal walls*

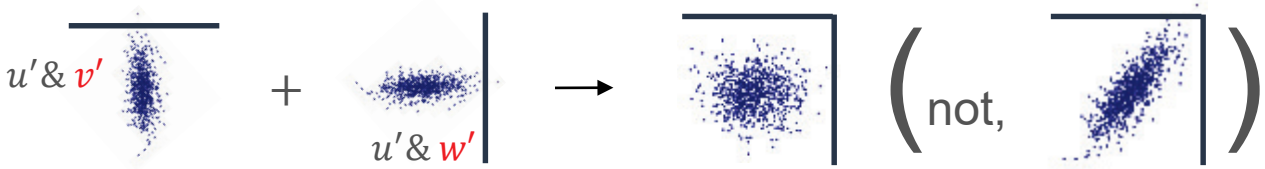

CONTENTS

Discussions

Overestimation of heat transfer in mixed convection with RANS turbulence models

– Heat transfer phenomena not included in RANS turbulence modeling

① Density gradient in the radial direction

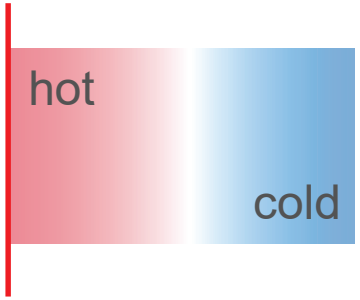

- ✓ Mean temperature gradient (← Reynolds averaging)
  ; Buoyancy production, $G_b = \beta \frac{\mu_t}{\mathrm{Pr}_t} (\nabla T \cdot \vec{g})$ is negligible in the vertical direction.
- ✓ In the developed region, axial mean $\nabla T \ll$ radial mean ∇T

② Flow characteristics near the corner regions

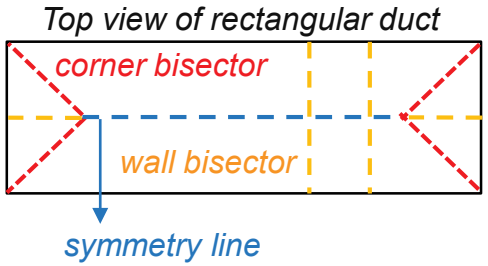

- ✓ Near wall distance
  → Influence of multiple walls is not considered.
- ✓ Reduced turbulence production near the corners from the experiment and DNS results

✓ More decrease of Reynolds shear stress;

① With heating

② Near corners

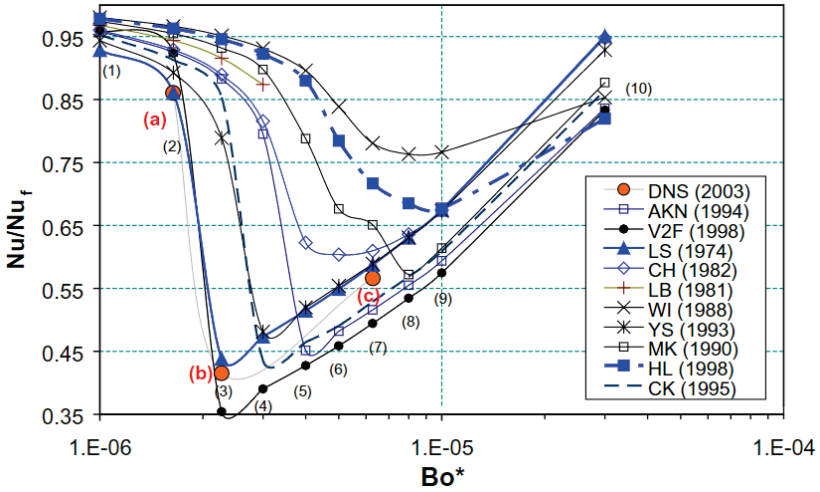

Influences of buoyancy on heat transfer in a tube from simulations using RANS turbulence models and DNS calculations [W. S. Kim et al., 2008]

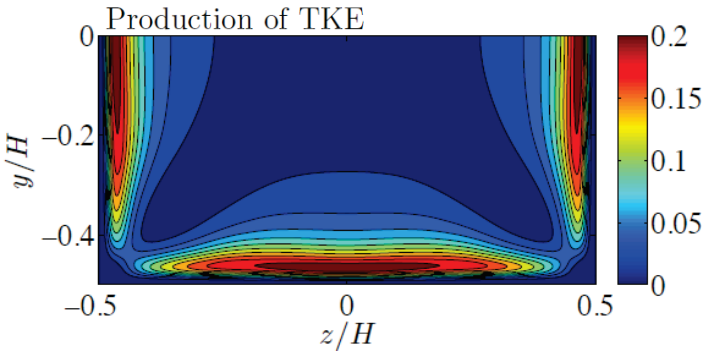

Distribution of turbulence production
[DNS, Marin et al. from Zhang et al., 2016]

Improvement of RANS turbulence model

Modification 1

; Turbulence production by the density-gradient induced vortex

- Magnitude; From the buoyancy production term, G_b
- Sign;
  ① Gravity-perpendicular velocity gradient direction; $\frac{\nabla u_x}{|\nabla u_x|} = \frac{-\nabla(\vec{U}\cdot\hat{g})}{|\nabla(\vec{U}\cdot\hat{g})|}$
  ② Density gradient direction

$$G_b = -\frac{\mu_t}{\mathrm{Pr}_t}(\nabla\bar{\rho}\cdot\vec{g})/\bar{\rho} \Rightarrow \boxed{G_{gperp} = -\frac{\frac{\mu_t}{\mathrm{Pr}_t}|\vec{g}|\left(\nabla\bar{\rho}\cdot\frac{-\nabla(U\cdot\hat{g})}{|\nabla(U\cdot\hat{g})|}\right)}{\bar{\rho}}}$$

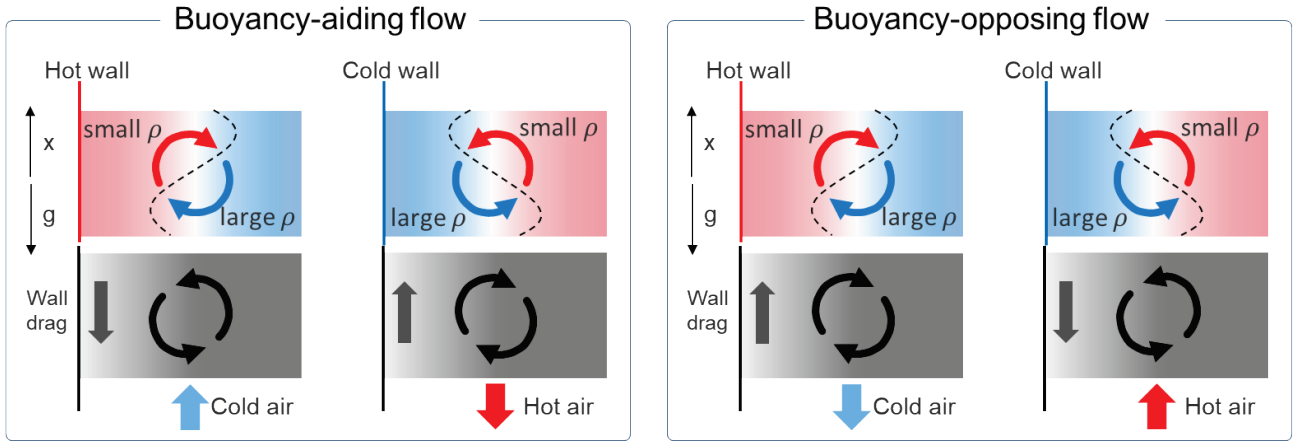

Modification 2

; **Derivation of additional term for the flow characteristics along the corner bisector**

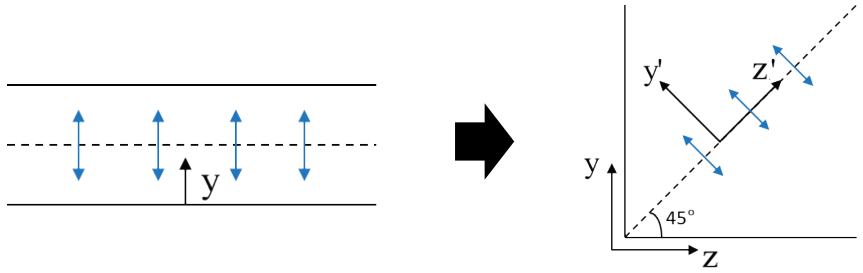

$$\rightarrow L^2\left(\nabla^2 f - 2C_{corner}\left|\frac{\partial^2}{\partial y\partial z}f\right|\right) - f = -\frac{\Pi_{ij}}{k} - \frac{\left[\overline{u_i u_j}/k - \frac{2}{3}\right]}{T}$$

for elliptic relaxation equation of V2F *k-ε* model

Flow characteristics near corner region in a rectangular duct

✓Corner bisectors ≈ line of symmetry ≈ wall bisectors

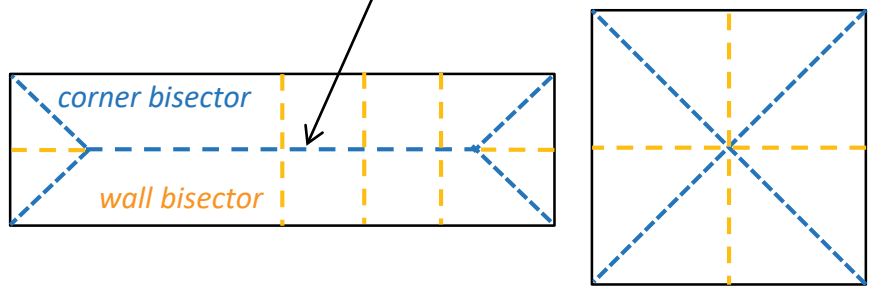

Improvement of RANS turbulence model

PhitF $k-\varepsilon$ model in OpenFOAM v.2012 (Laurence et al., 2004)

- Baseline model and modified model

Transport equations of baseline model

k;
$$\frac{\partial}{\partial t}(\rho k)+\nabla\cdot(\rho\vec{u}k)-\nabla^2\left(\rho\left(\nu+\frac{\nu_t}{\sigma_k}\right)k\right)=\rho G_k-\frac{2}{3}\rho(\nabla\cdot\vec{u})k-\frac{\rho}{T}k$$

ε;
$$\frac{\partial}{\partial t}(\rho\varepsilon)+\nabla\cdot(\rho\vec{u}\varepsilon)-\nabla^2\left(\rho\left(\nu+\frac{\nu_t}{\sigma_\varepsilon}\right)\varepsilon\right)=C_{\varepsilon1}\rho\frac{G_k}{T}-\frac{2}{3}C_{\varepsilon1}\rho(\nabla\cdot\vec{u})\varepsilon-C_{\varepsilon2}\frac{\rho}{T}\varepsilon$$

f;
$$-\nabla^2 f=-\frac{f}{L^2}-\left((C_{f1}-1)\frac{\varphi-\frac{2}{3}}{T}-\frac{C_{f2}G_k}{k}+C_{f2}\frac{2}{3}\nabla\cdot\vec{u}-\frac{2\nu(\nabla\varphi\cdot\nabla k)}{k}-\nu\nabla^2\varphi\right)\frac{1}{L^2}$$

φ;
$$\frac{\partial}{\partial t}(\rho\varphi)+\nabla\cdot(\rho\vec{u}\varphi)-\nabla^2\left(\rho\left(\nu+\frac{\nu_t}{\sigma_\varphi}\right)\varphi\right)=\rho f-\rho\varphi\left(\frac{G_k}{k}-\frac{2}{3}\nabla\cdot\vec{u}-\frac{2\nu(\nabla\varphi\cdot\nabla k)}{k\sigma_\varphi\varphi}\right)$$

$$T=\max\left(\frac{k}{\varepsilon},C_T\frac{\sqrt{\max(\nu,0)}}{\varepsilon}\right)$$

$$L=C_L\max\left(\frac{k^{1.5}}{\varepsilon},C_\eta\left(\frac{(\max(\nu,0))^3}{\varepsilon}\right)^{0.25}\right)$$

Transport equations of modified model

$$\frac{\partial}{\partial t}(\rho k)+\nabla\cdot(\rho\vec{u}k)-\nabla^2\left(\rho\left(\nu+\frac{\nu_t}{\sigma_k}\right)k\right)=\rho(G_k+G_b+G_{gperp})-\frac{2}{3}\rho(\nabla\cdot\vec{u})k-\frac{\rho}{T}k$$

$$\frac{\partial}{\partial t}(\rho\varepsilon)+\nabla\cdot(\rho\vec{u}\varepsilon)-\nabla^2\left(\rho\left(\nu+\frac{\nu_t}{\sigma_\varepsilon}\right)\varepsilon\right)=C_{\varepsilon1}\rho\frac{\left(G_k+C_{\varepsilon3}(G_b+G_{gperp})\right)}{T}-\frac{2}{3}C_{\varepsilon1}\rho(\nabla\cdot\vec{u})\varepsilon-C_{\varepsilon2}\frac{\rho}{T}\varepsilon$$

$$-\nabla^2 f=-2C_{corner}\left|\frac{\partial^2 f}{\partial y\partial z}\right|-\frac{f}{L^2}-\left((C_{f1}-1)\frac{\varphi-\frac{2}{3}}{T}-\frac{C_{f2}(G_k+G_b+G_{gperp})}{k}+C_{f2}\frac{2}{3}\nabla\cdot\vec{u}-\frac{2\nu(\nabla\varphi\cdot\nabla k)}{k}-\nu\nabla^2\varphi\right)\frac{1}{L^2}$$

$$\frac{\partial}{\partial t}(\rho\varphi)+\nabla\cdot(\rho\vec{u}\varphi)-\nabla^2\left(\rho\left(\nu+\frac{\nu_t}{\sigma_\varphi}\right)\varphi\right)=\rho f-\rho\varphi\left(\frac{(G_k+G_b+G_{gperp})}{k}-\frac{2}{3}\nabla\cdot\vec{u}-\frac{2\nu(\nabla\varphi\cdot\nabla k)}{k\sigma_\varphi\varphi}\right)$$

$$T=\max\left(\frac{k}{\varepsilon},C_T\frac{\sqrt{\max(\nu,0)}}{\varepsilon}\right)$$

$$L=C_L\max\left(\frac{k^{1.5}}{\varepsilon},C_\eta\left(\frac{(\max(\nu,0))^3}{\varepsilon}\right)^{0.25}\right)$$

Calculation conditions

OpenFOAM v.2012 (2020.12.)

— PhitF $k-\varepsilon$ turbulence model and with modifications

Calculation geometry

— Quarters of the geometry with symmetry planes (average y+ < 0.5)

— Solid part (for the stability of calculation near the corners)

Boundary conditions

— Temperature gradient on the outer wall

— Inlet average velocity with corresponding turbulence quantities

• Physical models (Steady condition)

	Fluid part	Solid parts
Solver	chtMultiRegionSimpleFoam (conjugate heat transfer)	
Thermo. type	heRhoThermo	heSolidThermo
Transport	k, μ; polynomial	k; constIso
Thermo	c_p; hPolynomial	c_p; hConst
Equation of State	PengRobinsonGas	rhoConst
Energy	sensibleEnthalpy	sensibleEnthalpy
Pr_t	0.85	-

• Used meshes for the calculation geometry (Depth x Width x Length)

	Mesh of fluid part	Mesh of total geometry
Cylinder	120x40x500 (Whole)	140x40x500 (Whole)
Aspect ratio = 6	20x60x1000 (Quarter)	25x65x1000 (Quarter)
Aspect ratio = 3	21x45x1000 (Quarter)	26x50x1000 (Quarter)
Aspect ratio = 1	30x30x1000 (Quarter)	35x35x1000 (Quarter)

• Example of the generated mesh (Aspect ratio = 3)

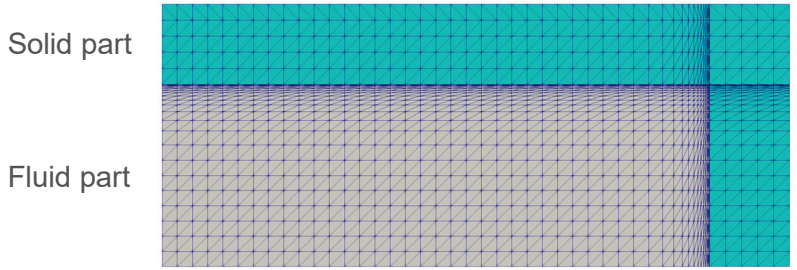

• Boundary conditions of properties of fluid

	Wall	Inlet	Outlet
U	fixedValue; 0	fixedValue	zeroGradient
k	fixedValue; 0	$\frac{3}{2}(IU_{in})^2$	zeroGradient
ε	epsilonWallFunction	$\frac{C_\mu^{3/4} k^{3/2}}{L}$	zeroGradient
f	fixedValue; 0	zeroGradient	zeroGradient
phit	fixedValue; 0	fixedValue; 0.66	zeroGradient
nut	nutUWallFunction	calculated	zeroGradient
p_rgh	fixedFluxPressure	zeroGradient	FixedMean

$I = 0.16\mathrm{Re}^{-1/8}, L = 0.07D_h$

Validation for modified turbulence model (1/2)

Comparison between the baseline and modified model (including density-gradient induced vortex)

- PhitF *k-ε* model in OpenFOAM v.2012
- $C_{corner} \rightarrow 1.6$

➢ Without heating (Case-2 from FROVE experiment)

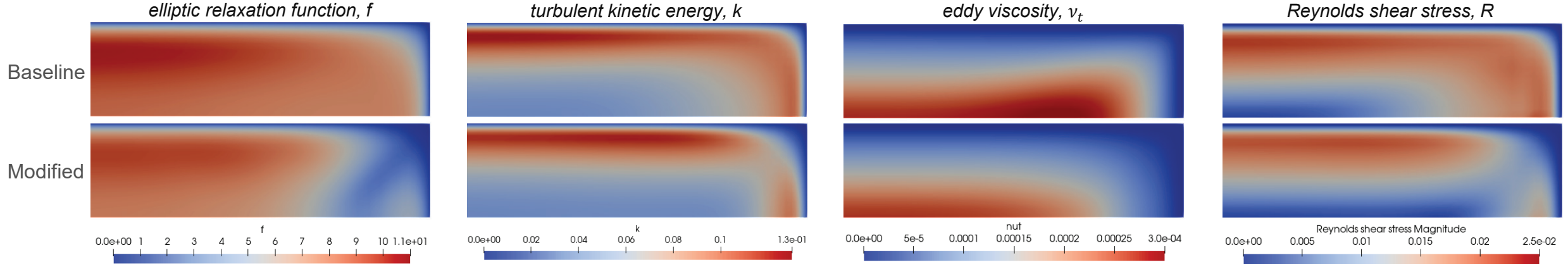

➢ In mixed convection (Case-9 from FROVE experiment); flow laminarization preceding near the corner

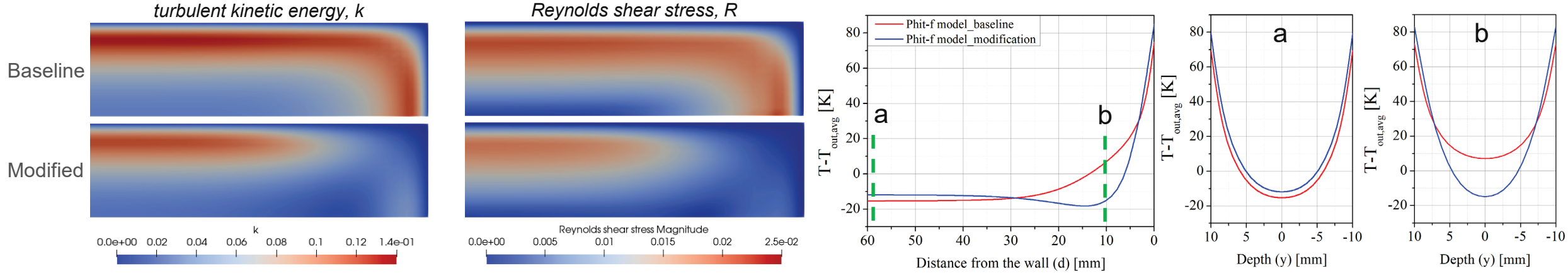

Validation for modified turbulence model (2/2)

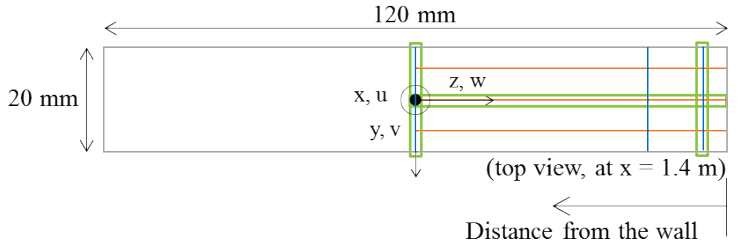

Comparison with the experimental data

- Modified PhitF *k-ε* model predicts the experimental data closely.
  - ✓ $C_{corner} = 1.4\ and\ 1.6$

Modified PhitF *k-ε* model; $L^2\left(\nabla^2 f - 2C_{corner}\left|\frac{\partial^2}{\partial x \partial y} f\right|\right) - f = -\frac{\Pi_{ij}}{k} - \frac{\left[\overline{u_i u_j}/k - \frac{2}{3}\right]}{T}$

- *Case-2 (Re=5500, ΔT=0K)*

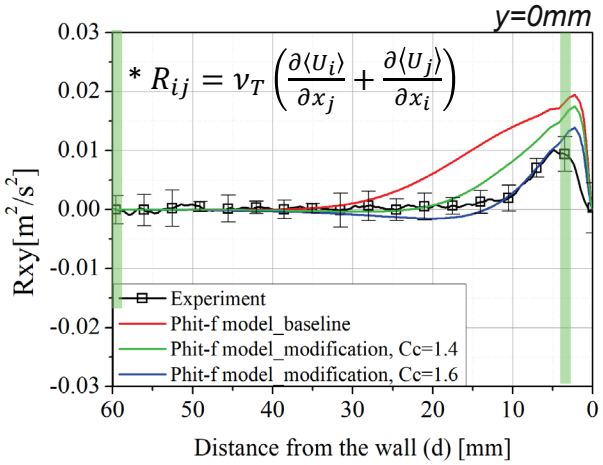

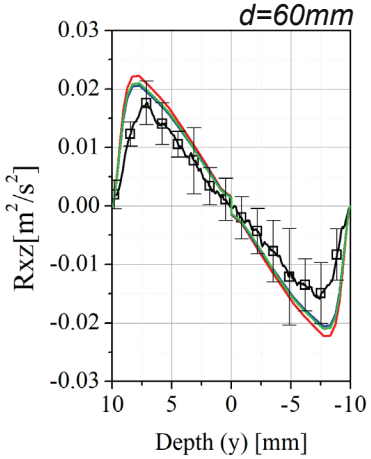

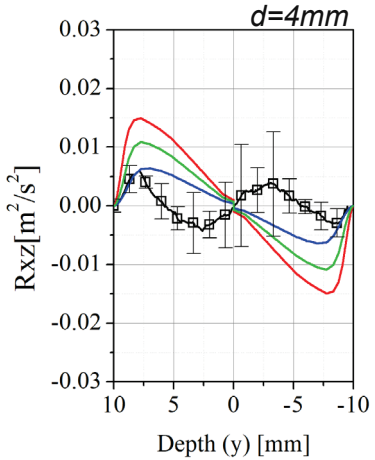

- *Case-9 (Re=5000, Re_b=4400, ΔT=81.5K)*

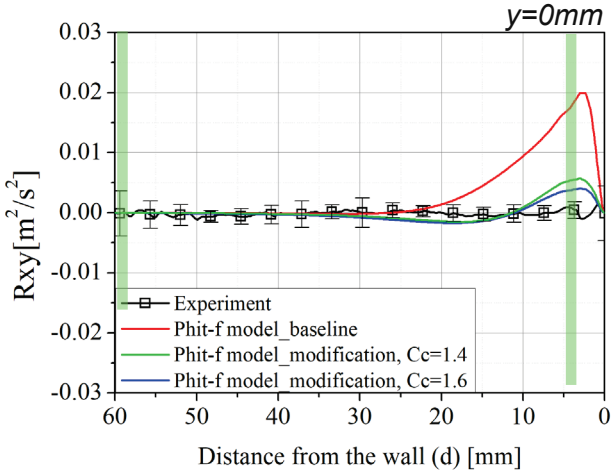

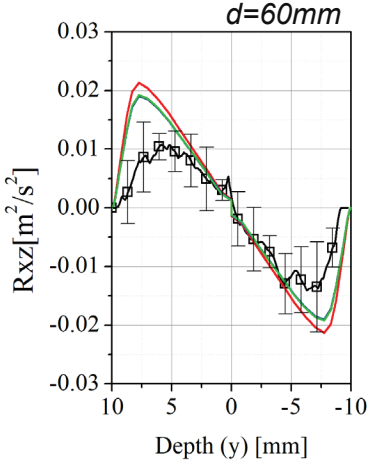

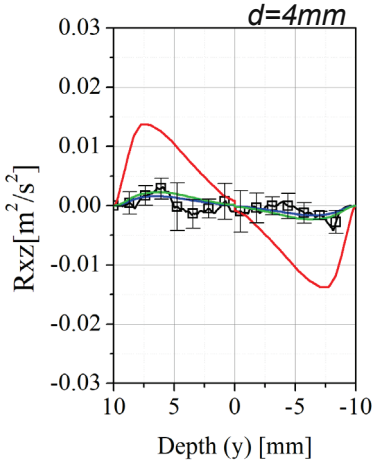

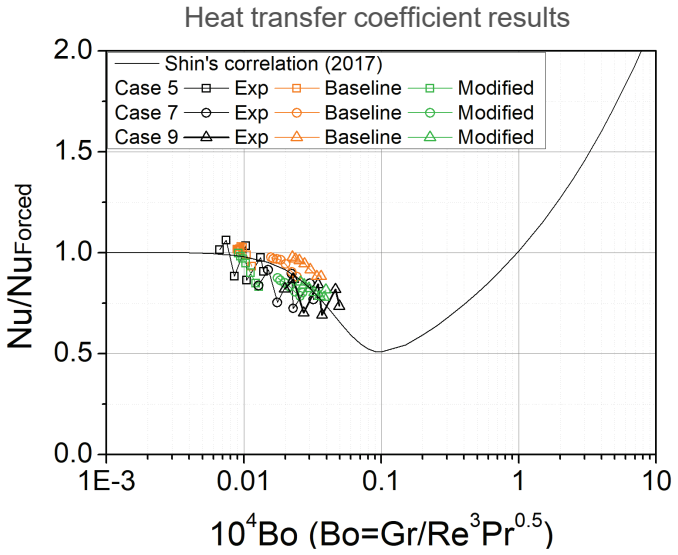

CONTENTS

Conclusions

Experimental researches

- Reduced turbulence production with lower plenum design
- Validation with turbulence quantities, not average velocity
- Physical insight with vortex motions

CFD analysis

- Inlet conditions for turbulence kinetic energy and its dissipation
- The papers that proposed famous turbulence models

✓ Validation process improves results and discussion.

Thank you!

kimsy@kaeri.re.kr

Nuclear hydrogen research team

Korea Atomic Energy Research Institute

Comparison with other experimental data

Experiment with rectangular riser in SNU

- ✓ The modified turbulence model shows improved prediction under conditions where heat transfer deteriorates.
  - RHEF experiment; 240mm x 40 mm x 4000mm (W x D x H)
  - FROVE experiment (this study); 120mm x 20 mm x 2000mm (W x D x H) (Heated test section)

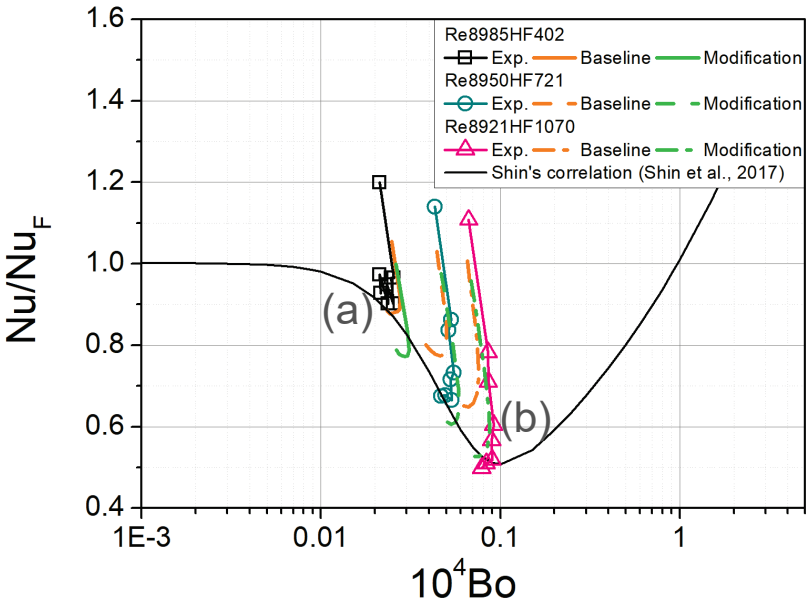

The heat transfer coefficient depending on the Bo with and without modification of turbulence model

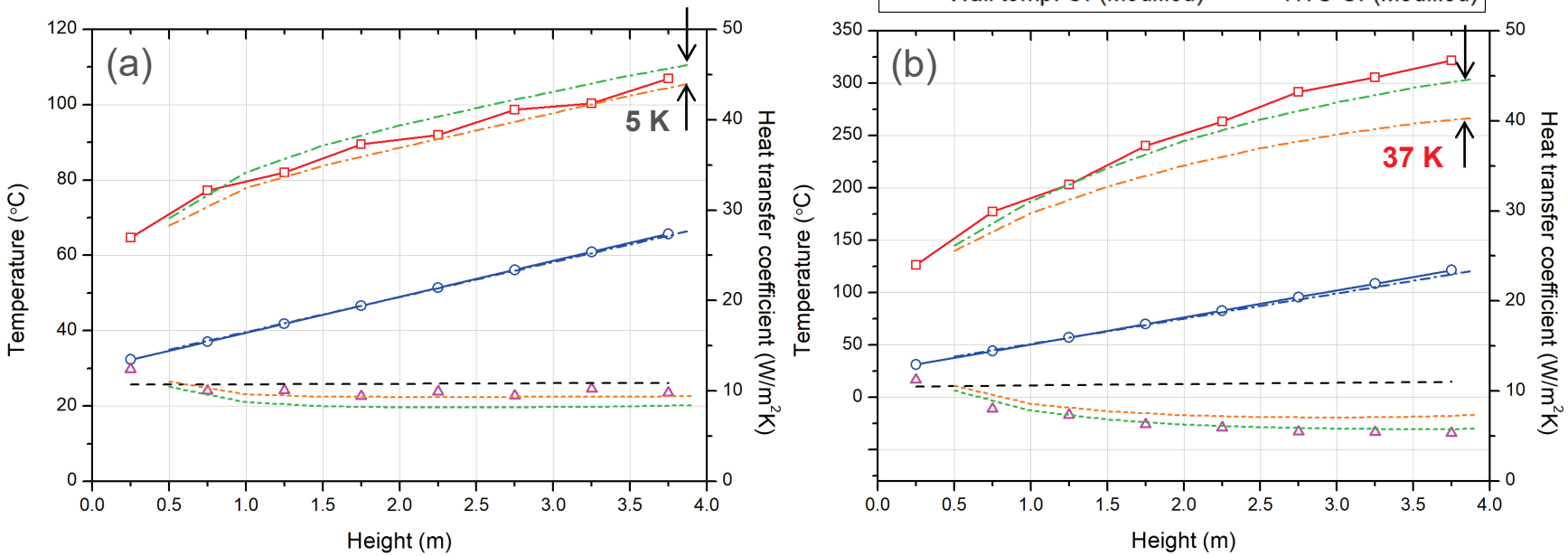

Experimental data and CFD analysis results with and without modification of turbulence model ; Re8985HF402 (left) and Re8921HR1070 (right)